AEDC-TR-70-168

JUN 22 1970

Copy 2

TIME-MARKING HIGH-SPEED FILM IN MULTIPLE-CAMERA INSTALLATIONS

H. T. Kalb and F. L. Crosswy

ARO, Inc.

June 1970

This document has been approved for public release and sale; its distribution is unlimited.

ARNOLD ENGINEERING DEVELOPMENT CENTER

AIR FORCE SYSTEMS COMMAND

ARNOLD AIR FORCE STATION, TENNESSEE

PROPERTY OF U. S. AIR FORCE
AEDC LIBRARY
F40600-69-C-0001

NOTICES

When U. S. Government drawings specifications, or other data are used for any purpose other than a definitely related Government procurement operation, the Government thereby incurs no responsibility nor any obligation whatsoever, and the fact that the Government may have formulated, furnished, or in any way supplied the said drawings, specifications, or other data, is not to be regarded by implication or otherwise, or in any manner licensing the holder or any other person or corporation, or conveying any rights or permission to manufacture, use, or sell any patented invention that may in any way be related thereto.

Qualified users may obtain copies of this report from the Defense Documentation Center.

References to named commercial products in this report are not to be considered in any sense as an endorsement of the product by the United States Air Force or the Government.

TIME-MARKING HIGH-SPEED FILM IN MULTIPLE-CAMERA INSTALLATIONS

H. T. Kalb and F. L. Crosswy
ARO, Inc.

This document has been approved for public release and sale; its distribution is unlimited.

FOREWORD

The work reported herein was sponsored by the Arnold Engineering Development Center (AEDC), Air Force Systems Command (AFSC), Arnold Air Force Station, Tennessee.

The work was accomplished by ARO, Inc. (a subsidiary of Sverdrup & Parcel and Associates, Inc.), contract operator of AEDC, AFSC, under Contract F40600-69-C-0001. The work was conducted under ARO Project No. BT6000 from January to May 1968. The manuscript was submitted for publication on June 18, 1969.

The authors acknowledge the significant contributions of P. L. Long in the design and development of the time and event signal generator. Acknowledgement is also made to G. F. Ford for his contribution in field testing the generator and analyzing results on film.

This technical report has been reviewed and is approved.

M. K. Kingery
Research Division
Directorate of Plans
and Technology

Harry L. Maynard
Colonel, USAF
Director of Plans
and Technology

ABSTRACT

The general time-event correlation problem for high-speed (10,000-frames/second), motion analysis cameras is discussed. The specific optics, sensitometry, and electronics problems involved in placing precise time and event marks on high-speed film, in addition to the design and development of an operational time and event signal generator, are discussed. The generator features a tuning fork time standard, integrated circuit timing logic that can furnish independent time and event signals for up to 15 cameras. A current ramp-film density wedge generator is presented as a novel method for relating time-mark lamp current amplitude to film-mark density. Recently developed, solid-state, light emitting diodes (LED) were investigated for application to the time-mark problem. The LED proved capable of providing time-marking pulses at rates in excess of 200 kHz. A technique for analyzing a waveform to operationally test the neon lamp timing circuit is evaluated.

CONTENTS

		Page
	ABSTRACT	iii
	NOMENCLATURE	vii
I.	INTRODUCTION	1
II.	FUNDAMENTAL CONSIDERATIONS	
	2.1 Transmission Line Characteristics	2
	2.2 Effect of Source, Transmission Line, and Load Characteristics on Pulse Signal Propagation	6
	2.3 Neon Lamp Characteristics	8
	2.4 Film-Marking Problem	9
	2.5 Lamp Voltage Waveform Analysis	11
	2.6 Undesirable Lamp Ionization Modes	12
	2.7 Extreme Cases of Delay in Lamp Ionization	13
	2.8 Improvement of Pulse Transmission through Lengthy Cables	14
	2.9 Semiconductor Lamp	20
III.	DESCRIPTION OF AN OPERATIONAL TIME-MARK GENERATOR	23
IV.	TIMING LIGHT INTENSITY/FILM-MARK DENSITY RELATIONSHIP	
	4.1 Photographic Properties of Film	25
	4.2 Light Intensity	26
	4.3 Definition of a Timing Mark	27
	4.4 Problem of Establishing a Qualitative Relation between Time-Mark Density and Lamp Current/Time Pulse	28
	4.5 Current Ramp-Density Wedge Generator	29
V.	SUMMARY OF RESULTS AND CONCLUSIONS	31
	REFERENCES	32

APPENDIXES

I. ILLUSTRATIONS

Figure

1. Speed-Time Characteristics of a High-Speed Camera (400 ft of Supply Film) . . . 37
2. High-Speed Camera Time and Event Signal Generator . . . 38

Figure		Page
3.	Analytical Model of a Transmission Line	39
4.	Open-Circuited Transmission Line Output Voltage Waveforms	40
5.	Neon Lamp Driving Voltage Waveforms	41
6.	Neon Lamp Ionization Curves in Time Comparison with Three Representative V_L Waveforms	42
7.	Timing Lamp Installation Model and Equivalent Circuit	43
8.	General Form of Lamp Voltages Commonly Found in Timing Light Circuits Using Neon Lamps	44
9.	Lamp Voltage-Current Characteristics for Four $R_b\Delta C$ Time Constants	45
10.	Lamp Current versus Lamp Intensity	45
11.	Undesirable Delayed Ionization Mode of the Neon Lamp	46
12.	Extreme Lamp Ionization Delay	47
13.	Switching Transistor at the Camera	48
14.	Effect of Keep Alive in Reduction of Lamp Ionization Delay	49
15.	Lamp volt-amp Waveform, Lamp Driven with Keep Alive	49
16.	Neon Lamp Relaxation Oscillation Problem	50
17.	Comparison of the Dynamic Breakdown Voltages for NE51 and NE51H Lamps with Large $R_b\Delta C$ Time Constants	50
18.	Comparison of Conventional Circuit to Dynamic Ballast	51
19.	Solid-State Light Emitting Diode Driver Circuit	55
20.	Waveforms for a Gallium Arsenide Phosphide Light Emitting Diode Driven at the Terminal End of a 300-ft RG62 Transmission Line	56
21.	Gallium Arsenide Phosphide Diode Driven at 90-MHz Rate	58

Figure		Page
22.	Block Diagram of a 15 Camera Timing Light Generator	59
23.	Timing Logic Circuit	60
24.	General Characteristic Curve for Photographic Film	61
25.	Current Ramp-Density Wedge Generator	62
26.	Series of Lamp Current Pulses of Linearly Increasing Amplitude	63
27.	Density versus Lamp Current for 7258 Color Reversal Film	64
28.	Samples of Timing Marks Produced with and without Light Collimating Devices	65

II. NEON GLOW LAMP CHARACTERISTICS 66

NOMENCLATURE

C	Capacitance per unit length of transmission line
D	Schematic symbol for a diode
d	Total length of a transmission line
dbm	Signal power into 50 ohms with 1-mw reference
E_z	Zenner diode voltage
G	Leakage conductance per unit length of transmission line
I_{cex}	Collector to emitter current, transistor reverse biased
I (x, s)	Laplace transform of i (x, t)
i (x, t)	Current at any point along a transmission line
L	Inductance per unit length of transmission line
LED	Light emitting diode
PRR	Pulse repetition rate of lamp, pulses per unit time
PPS	Pulses per second
Q	Electric charge or schematic symbol for a transistor

R	Resistance per unit length of transmission line
R_b	Ballast (current limiting) resistance
R_L	Load resistance
R_o	Lossless transmission line characteristic resistance
s	Laplace transform variable
t_D	Time delay in lamp ionization, relative to V_s step function
t_d	Propagation delay time of a transmission line of specified length
t_p	Signal generator pulse duration time
V_B	Dynamic breakdown voltage of neon lamp
V_{bef}	Transistor base to emitter voltage, transistor forward biased
V_{ic}	Initial condition voltage across the lamp
$V_L(t)$	Voltage across neon lamp as a function of time
V_m	Voltage drop across ionized neon lamp, maintaining voltage
V_s	Peak signal generator voltage
$V_s(t)$	Signal generator time function voltage
$V(x, s)$	Laplace transform of $v(x, t)$
ΔV	$\Delta V = V_B - V_M$
v	Transmission line propagation velocity
$v(x, t)$	Voltage at any point along a transmission line
Z_L	Load impedance
Z_s	Signal generator output impedance
Z_o	Transmission line characteristic impedance
γ	Photographic film parameter, gamma
ϵ	Permittivity of insulating material
ϵ_o	Permittivity of free space
μ	Permeability of insulating material
μ_o	Permeability of free space
τ	Time constant

SECTION I
INTRODUCTION

High-speed cameras ($\leq$ 10,000-frames/second) are extensively used for photographic motion analysis in various test cells at the Arnold Engineering Development Center (AEDC). However, the motor-driven cameras presently used do not run at a constant frame rate, so that time correlation of the event recorded on the film is not directly available. For example, Fig. 1 (Appendix I) shows that the speed versus time characteristics of a typical high-speed camera have a nonconstant frame rate. To correlate the events recorded on the film with elapsed test time, neon lamps (recently, solid-state light emitting diodes have also been used) mounted inside the camera and driven with precisely timed current pulses can be used to mark the film margins. In some instances, it is also desirable to place a special mark on the film to coincide with a particular event during the test.

Multiple-camera installations are often used to record the test data from several different locations in the test cell, and it is not uncommon for a dozen cameras to be used concurrently. Frequently, the cameras are run in sequence, at different speeds, to satisfy the particular test requirements. The cameras are usually mounted inside protective enclosures because of the extreme environmental test conditions in the test cell. A typical test might involve high altitude pressure simulation with a captive test firing of a rocket engine. The cameras are usually operated remotely, from within a control room, where direct view of or access to the cameras immediately before or during the test is not possible. The control room may be located several hundred feet from the test cell. All these conditions contribute complexities to the problem of placing time and event markers on the high-speed film.

Successful placement of time marks on high-speed film requires careful consideration of the electrical characteristics of the light source, the pulsed power supply, and the intervening transmission line. It is also important to investigate the relationships between film-mark density and the exposure parameters: film speed, light source current, and pulse width.

The purpose of this report is (1) to furnish a description of a recently developed time and event signal generator for multiple high-speed camera installations, (2) to present an electrical model of the neon lamp circuit for analysis purposes, (3) to illustrate the electrical characteristics of the neon lamp circuit by oscilloscope photographs, (4) to illustrate a method for pretest checkout of the neon lamp circuits, (5) to describe a method for applying controlled variable density marks to a

high-speed film so that an optimum mark density for that particular film may be chosen, and (6) to present data using a recently developed solid-state light emitting diode which illustrates the significant advantages of the diode as compared to the neon lamp for time and event signal generator purposes.

SECTION II
FUNDAMENTAL CONSIDERATIONS

A schematic representation of a single time and event signal system is shown in Fig. 2. This system is formed by interconnection of three components: (1) the signal generator, (2) the transmission line, and (3) the neon lamps located inside the high-speed camera. The transmission line characteristics must be considered when time and event voltage pulses are to be transmitted from the signal generator to the neon lamps. The ballast resistor, R_b, shown in Fig. 2, limits the current to the neon lamp following ionization of the lamp.

2.1 TRANSMISSION LINE CHARACTERISTICS

Any one of several types of transmission line could be used with the time and event signal generator:

1. Parallel-wire lines,
2. Strip-line configuration,
3. Wire over ground plane, and
4. Coaxial cable.

Despite the fact that all transmission lines have certain general properties in common, the coaxial cable type is preferred when specific transmission characteristics are compared. Coaxial cable was selected for the time and event generator, and the following discussions pertain to this type of transmission line.

An analytical model of a transmission line is shown in Fig. 3, along with the parameters and variables describing its characteristics (Ref. 1).

$$L \frac{\partial i(x,t)}{\partial t} + Ri(x,t) = -\frac{\partial v(x,t)}{\partial x} \tag{1}$$

$$C \frac{\partial v(x,t)}{\partial t} + Gv(x,t) = -\frac{\partial i(x,t)}{\partial x} \tag{2}$$

Now, assuming zero initial conditions, the Laplace transformed transmission line equations become:

$$(Ls + R)\, I(x,s) = -\frac{\partial V(x,s)}{\partial x} \tag{3}$$

$$(Cs + G)\, V(x,s) = -\frac{\partial I(x,s)}{\partial x} \tag{4}$$

where $I(x, s)$ and $V(x, s)$ are the Laplace transforms of $i(x, t)$ and $v(x, t)$, respectively. With algebraic manipulation, Eqs. (3) and (4) can be put into the form:

$$\frac{\partial^2 I(x,s)}{\partial x^2} - (Ls + R)\,(Cs - G)\, I(x,s) = 0 \tag{5}$$

$$\frac{\partial^2 V(x,s)}{\partial x^2} - (Ls + R)\,(Cs + G)\, V(x,s) = 0 \tag{6}$$

The complementary solutions of Eqs. (5) and (6) are:

$$I(x,s) = A_1 e^{-nx} + B_1 e^{nx} \tag{7}$$

$$V(x,s) = A_2 e^{-nx} + B_2 e^{nx} \tag{8}$$

where A_1, A_2, B_1, and B_2 are functions of s and are determined by the applicable boundary conditions and

$$n = \sqrt{(Ls + R)\,(Cs + G)} \tag{9}$$

If a signal generator voltage, $V_s(t)$, is impressed on a transmission line of length, d, terminated in the impedance, Z_o and Z_L, the Laplace transformed expressions for $v(x, t)$ and $i(x, t)$ are $V(x, s)$ and $I(x, s)$, respectively (Ref. 1):

$$V(x,s) = \frac{\left(\frac{Z_o}{Z_o + Z_s}\right)\left[e^{-nx} - \left(\frac{Z_o - Z_L}{Z_o + Z_L}\right)e^{-n(2d - x)}\right] V_s(s)}{1 - \left(\frac{Z_o - Z_s}{Z_o + Z_s}\right)\left(\frac{Z_o - Z_L}{Z_o + Z_L}\right) e^{-2nd}} \tag{10}$$

$$I(x,s) = \frac{\left[\frac{1}{Z_o + Z_s}\right]\left[e^{-nx} + \left(\frac{Z_o - Z_L}{Z_o + Z_L}\right) e^{-n(2d-x)}\right] V_s(s)}{1 - \left(\frac{Z_o - Z_s}{Z_o + Z_s}\right)\left(\frac{Z_o - Z_L}{Z_o + Z_L}\right) e^{-2nd}} \tag{11}$$

where Z_o is the characteristic impedance of the transmission line and is given by:

$$Z_o = \sqrt{\frac{Ls + R}{Cs + G}} \tag{12}$$

Equations (10) and (11) are the Laplace transformed expressions for the voltage and current at any point, x, along the line at any time, t, following the application of the signal generator voltage, $V_s(t)$.

Equations (10) and (11) can be expressed in terms of attractive multiple reflections by expanding the denominators in a power series and simplifying:

$$V(x,s) = \frac{Z_o V_s(s)}{Z_s + Z_o}\left[e^{-nx} - Ne^{-n(2d-x)} + MNe^{-n(2d+x)} - MN^2e^{-n(4d-x)} + \ldots\right] \tag{13}$$

$$I(x,s) = \frac{V_s(s)}{Z_s - Z_o}\left[e^{-nx} + Ne^{-n(2d-x)} + MNe^{-n(2d+x)} - MN^2e^{-n(4d-x)} + \ldots\right] \tag{14}$$

where M is the signal generator reflection coefficient given by

$$M = \frac{Z_o - Z_s}{Z_o + Z_s} \tag{15}$$

and N is the load impedance reflection coefficient given by

$$N = \frac{Z_o - Z_L}{Z_o - Z_L} \tag{16}$$

The first term in Eqs. (13) and (14) represents the generator voltage and current waveform, respectively, traveling toward the load, whereas the second term represents a reflected wave from the load traveling toward the generator. Each succeeding odd and even term represents a re-reflected wave from the generator impedance and load impedance, respectively. Equations (13) through (16) show that voltage and current reflections with attendant signal distortion can be eliminated by matching the impedances of the generator and load to the transmission line characteristic impedance:

$$Z_s = Z_o = Z_L \tag{17}$$

The series resistance and shunt conductance of the relatively short lines (<400 ft) used with the time and event signal generator can be assumed to be zero for all practical purposes. Therefore, the characteristic impedance expression simplifies to

$$Z_o = R_o = \sqrt{\frac{L}{C}}\ \text{ohm} \tag{18}$$

and the velocity with which the wave travels along the line for the lossless transmission line is given by

$$v = \frac{s}{n} = \frac{1}{\sqrt{LC}}\ \text{m/sec} \tag{19}$$

The L and C parameters of a transmission line are functions of the geometry of the line. Application of Gauss's law to the coaxial transmission line geometry and subsequent calculation yields the capacitance per unit length:

$$C = \frac{2\pi\epsilon}{\ln b/a}, \frac{\text{farad}}{\text{meter}} \tag{20}$$

where b is the diameter of the outer cylindrical conductor, a is the diameter of the inner cylindrical conductor, and ϵ is the permittivity of the insulating material between the conductors. Application of the Biot-Savart law and subsequent calculation yields the external inductance per unit length for the coaxial transmission line

$$L = \frac{\mu}{2\pi} \ln b/a, \frac{\text{henry}}{\text{meter}} \tag{21}$$

where μ is the permeability of the insulating material.

Substitution of Eqs. (20) and (21) into Eq. (18) shows that the characteristic impedance of the lossless line is dependent on the constants ϵ and μ as well as the geometry of the line

$$R_o = \frac{\ln b/a}{2\pi} \sqrt{\frac{\mu}{\epsilon}} \text{ ohm} \tag{22}$$

Substitution of Eqs. (20) and (21) into Eq. (19) shows that the propagation velocity is dependent only on the constants ϵ and μ

$$v = \frac{1}{\sqrt{\epsilon\mu}} \text{ meters/sec} \tag{23}$$

For air insulating material, the constants μ and ϵ are the same as the free-space values for all practical purposes

$$\mu_o = 4\pi(10^{-7}) \text{ henry/meter}$$

$$\epsilon_o = [36\pi(10^9)]^{-1} \text{ farad/meter} \tag{24}$$

therefore,

$$v = 3(10^8) \text{ meters/sec} \tag{25}$$

or

$$\tau = \frac{1}{v} = 1.05 \text{ nsec/ft} \tag{26}$$

where τ is the delay constant.

For the polyethylene insulated coaxial cables used with the time and event signal generator, the time delay constant is given by

$$\tau = \sqrt{\epsilon\mu} = (\sqrt{2.3})\,(1.05) \text{ nsec/ft} \approx 1.6 \text{ nsec/ft} \tag{27}$$

where ϵ is the permittivity and μ is the permeability of polyethylene.

2.2 EFFECT OF SOURCE, TRANSMISSION LINE, AND LOAD CHARACTERISTICS ON PULSE SIGNAL PROPAGATION

From Eqs. (13) through (16), it can be seen that it is desirable to match the signal generator and load impedance to the transmission line characteristic impedance to prevent signal distortions caused by multiple reflections. However, impedance matching is not practical when using neon lamps in a time and event signal generator, as shown in Fig. 2, since the ballast resistor required to limit lamp current is large compared to the line R_o, and the effective impedance of the lamp varies over wide limits as the lamp is driven from its "off" to its "on" condition. The condition that prevails with the system shown in Fig. 2 is (before ionization of the neon lamp,

$$R_b \gg R_o \text{ and } Z_L \gg R_o \tag{28}$$

where R_b is the resistance of the ballast resistor, and Z_L is the effective impedance of the neon lamp. Under the conditions set forth in Eq. (28), the fast signal propagation capabilities of the transmission line are not exploited, and the line is equivalent to a lumped capacitance, ΔC. This equivalent lumped capacitance, for a line length d, is given by (Ref. 2)

$$\Delta C = \frac{T_d}{R_o}\left(1 - \frac{R_o^2}{R_b^2}\right) \text{farad } T = \frac{1}{v} \tag{29}$$

where T is the delay constant (T ≈ 1.6 nsec-ft for the polyethylene coaxial cable used).

The $R_b \Delta C$ time constant then dictates the rate of rise of the driving voltage across the neon lamp. This rate of rise along with the ionization and deionization times of the neon lamp then determines the maximum repetition rate at which the lamp can be driven. The time function voltage, $V_L(t)$, across the lamp (before lamp ionization) in response to a step function signal generator voltage, V_s, is approximated by:

$$V_L(t) = V_s\,(1 - e^{-t/\Delta C\, R_b}) \tag{30}$$

where $R_b \gg Z_s$.

Equation (30) closely predicts the voltage waveform across the lamp before lamp ionization. The effective lamp impedance before ionization is quite large (>10 megohms) and appears as an open circuit for all practical purposes. However, when the lamp ionizes, its effective impedance is quite low (<4000 ohms), Ref. 3. Figure 4 shows the voltage waveform at the output of 400 ft of RG58 cable in response to the signal

generator voltage, $V_s(t)$, input (approximately 1-μsec rise time) for three different values of ballast resistance, R_b. The voltage waveforms can be seen to follow that predicted by Eq. (30).

Figure 5 shows three superimposed traces of the voltage waveform: (1) at the terminal end of an open circuited 400-ft transmission line with an R_o of 50 ohms and a ΔC of 0.012 μf, (2) the same line terminated in a neon lamp, and (3) the transmission line replaced by a lumped 0.012-μf capacitor in parallel with the neon lamp. It is noted that there is precise correspondence in the lamp waveform under conditions (2) and (3). The same value of R_b was used in the three traces.

It was experimentally confirmed that, irrespective of the cable length and the type of neon lamp (high brightness or standard), the voltage waveform could be adequately described by Eqs. (29) and (30). It was further determined that the voltage seen at the sending end of the transmission line was identical in appearance to that seen across the lamp at the receiving end. The significance of this is that in camera installations where lengthy cable lines exist between the generator and camera, appreciable delays in lamp ionization can occur. This delay cannot be accurately predicted on the basis of Eqs. (29) and (30) alone, because of the variable ionization characteristics of each lamp. It will be seen, however, that the delay can be accurately determined by observation of the lamp voltage waveform leading edge, observed at the position of the timing light generator. One additional point of interest is the residual voltage that can remain across the ΔC between timing pulses. This voltage is an initial condition voltage, V_{ic}, and its inclusion modifies Eq. (30) to:

$$V_L(t) = V_{ic} + (V_s - V_{ic})(1 - e)^{-t/R_b \Delta C)} \tag{31}$$

The initial condition arises in practice when a "bias" voltage is applied to the lamp electrodes between driving pulses or a large impedance is offered the ΔC once the lamp voltage drops below the minimum maintaining voltage for ionization at the termination of a driving pulse. The time delay in lamp starting can be expressed as:

$$t_D = \left[(R_b \Delta C)\right]\left[\ln\left(\frac{V_s - V_{ic}}{V_s - V_B}\right)\right]\text{sec} = \left[\left(\frac{R_b T_d}{R_o}\right)\right]\left[\ln\left(\frac{V_s - V_{ic}}{V_s - V_B}\right)\right]_{\text{sec}} \tag{32}$$

All parameters can be determined except V_B, which is defined as the dynamic breakdown voltage of the neon lamp and can be shown as a locus of points when plotted against a time scale; this plot is called the ionization curve of the lamp.

2.3 NEON LAMP CHARACTERISTICS

Dynamic breakdown voltage characteristics for a neon lamp can be experimentally determined by applying a ramp function driving voltage to the lamp and then plotting the lamp breakdown voltage versus the time to breakdown (time referenced to start of the ramp). It has been found that these characteristics can vary significantly among lamps of the same type. Also, aging effects can greatly alter the characteristics of the neon lamp. However, dynamic breakdown characteristics in graphical form are quite useful for estimating the time delays to be expected in neon lamp ionization following the application of a step function voltage by the signal generator. This time delay limits the rate at which the timing marks can be applied to the motion-picture film.

Typical neon lamp (new) ionization curves (A through E, Fig. 6) were plotted for lamps, in total darkness, driven at three specified pulse repetition rates, with zero initial condition voltage applied. Curves F and G apply to an NE51 standard brightness lamp. All remaining curves apply to the NE51H high brightness lamp. It will be shown that the intersection of the lamp ionization curve with the applied voltage time-function plot adequately defines the firing point of the timing lamp and describes the delay time in lamp starting relative to the initiation of the driving pulse, V_S (applied to the input of the transmission line). It will also be shown that a break in the voltage waveform across the lamp viewed on an oscilloscope corresponds to this point of intersection of the two curves and represents the dynamic breakdown voltage of that particular lamp in its particular environment.

Curves B, D, and C (Fig. 6) show ionization values for the same lamp driven at different pulse repetition rates (PRR) of 10 and 100 Hz and 1 kHz, respectively. Over the time scale depicted, it is noted that the dynamic breakdown voltage at the slower PRR is substantially higher than the faster PRR. If the time scale of Fig. 6 were expanded, it would be noted that curves B and D approach a common value of 120 volts in several milliseconds. Curve C was found to remain below this value because of the 1-msec lapsed time between pulses. Curve A was plotted using a neon lamp other than the one used to plot curve C and illustrates the variation in characteristics to be expected for lamps of the same type. Curve G illustrates the ionization values for an "aged" NE51 lamp; curve F applies to a new NE51 lamp.

Curves 1, 2, and 3 in Fig. 6 represent typical driving voltage waveforms, $V_L(t)$, across a neon lamp for two different cable lengths, d, and two different initial condition voltages, V_{ic} with a step function driving voltage, V_S, applied to the transmission line. These curves, along with curves A through G, can be used to estimate lamp ionization delay time.

Curve 1 represents $V_L(t)$ across a nonionized neon lamp for $\Delta CR_b = 13\,\mu sec$ and $V_{ic} = 0$. This would be typical of a 30-ft RG58U cable, $\Delta C = 0.001\,\mu f$, and an R_b of 13 KΩ. Curve 2 represents $V_L(t)$ for a ΔCR_b of $130\,\mu sec$, $V_{ic} = 0$, d = 450 ft of RG58U, and R_b = 16 KΩ. Curve 3 has the same time constant as curve 2, but $V_L(t)$ differs in that an initial condition, V_{ic}, of 50 volts exists across the lamp.

Comparing the points of intersection of curves 2 and 3 with a given lamp ionization curve illustrates how V_{ic} can reduce lamp starting delay. A comparison of curve 1 with curve 2 demonstrates the lamp ionization delay caused by long cables. A comparison of a given $V_L(t)$ curve with curves B, D, and C illustrates the increasing delay time in lamp ionization at the slower pulse repetition rates.

The intercepts of curves 1 through 3 with the vertical line at $100\,\mu sec$ represent the terminal voltage values of $V_L(t)$ for a V_s driving pulse $100\,\mu sec$ in duration. In the examples given, all lamps would fire before the termination of a 100-sec pulse, but considerable variance would be experienced in the lamp current time plot.

Extreme time constants as long as 500 sec would be considered not uncommon in certain installations. Ionization curves of aged neon lamps would reflect increasing dynamic breakdown voltage values, as seen by curve G.

Certain lamps do not exhibit a repeatable ionization value when driven by a periodic pulse train. The dynamic breakdown voltage varies in a random fashion from pulse to pulse. This erratic firing behavior (for one lamp) has been illustrated by the cross-hatched region marked E. This region can be considered to represent an infinite number of possible breakdown voltage values. For a given installation with a characteristic $V_L(t)$, the erratic firing lamp will be observed to ionize at all points along the portion of the $V_L(t)$ curve contained within the E region. The effective area of the E region varies between lamps of the same type, with PRR (reduced area at higher PRR), hours of prestabilizing operation and because of lamp "dark" effect.

2.4 FILM-MAKING PROBLEM

The preceding section indicated how the transmission line, lamp ballast resistance, R_b, and signal generator driving pulse voltage, V_s, are interrelated to produce a delayed rise in voltage, $V_L(t)$, across the lamp. It was stated that a timing lamp installation model such as shown

in Fig. 7a could be simplified to that shown in Fig. 7b, where the concept of excess capacitance ΔC could be used to replace the transmission line. Note: The expression ΔC is retained throughout the report to emphasize that distributed capacitance is involved; Eq. (29) permits this capacitance to be treated as a lumped equivalent value as long as $R_b \geq 4\ R_o$. This concept must be reexamined in terms of the termination impedance at both ends of the line at any time a current or voltage change along the line is experienced. The neon lamp ionization curve was shown to be subject to a wide variation in dynamic breakdown voltages, particularly for V_s time periods shorter than 25 μsec.

The lamp possesses other characteristics which affect its use as a timing light, such as (1) its constant voltage nonlinear resistance nature, (2) the "dark effect", and (3) the tendency for the lamp electrodes to sputter (lamp darkening).

Ideally, a controlled amplitude-time pulse of current through the lamp is desired to reliably produce a timing mark on film. The pulse of light, proportional to the lamp current, should be optically coupled to the film in a manner that will minimize detrimental effects caused by variation among cameras, in light slit dimensions, and/or poor collimation of light and lamp bulb darkening. Finally, the rapid variations in frame rate of the film affects the exposure time, and further, the emulsion properties of the film must also be considered. Each of these problem areas will be discussed.

It is pertinent at this point to consider some of the characteristics of the lamp voltage waveforms encountered with generators containing the R_b ballast resistance at the sending end of the transmission line. Earlier, it was shown that a large value of R_b in combination with a lengthy line could produce objectionable time delays in lamp starting. This would, in turn, cause variations in the time duration of the light pulse from the lamp. Ideally, this problem would be alleviated if R_b plus the signal generator output impedance could be made to approach the characteristic impedance of the cable. Unfortunately, rapid ionization of the neon lamp requires a considerably larger voltage than the sustaining voltage required across the lamp, once the lamp is ionized, to produce the required current to achieve the desired light intensity. The size of R_b is dictated then by the magnitude of V_s and the desired level of lamp current. For example, for V_s = 375 volts, 8 ma of current requires $R_b \approx 33\ K\Omega$, and 23 ma of current requires $R_b \approx 12\ K\Omega$. By contrast, it will be shown that with the solid-state light diode, impedance matching is not a problem, and the ideal current pulse is indeed achieved, even at pulse repetition rates in excess of 200,000 PPS.

2.5 LAMP VOLTAGE WAVEFORM ANALYSIS

A technique has been developed whereby an operational checkout of a timing light installation using neon lamps can easily and quickly be performed. Figure 8 presents the general form of lamp voltages commonly found in timing light circuits. Figure 8a shows a lamp driven by a very short cable where the line capacitance is small. Here good definition of the voltage pulse can be seen. The initial condition voltage is zero, and the rise and fall character of the pulse is clearly evident. The lamp dynamic breakdown voltage approaches the driving pulse voltage (375 volts), and the delay time in reaching the breakdown voltage is small. At the termination of the pulse, the voltage across the lamp quickly drops to zero as small line capacitance is present for charge retention. The midsection waveform, of constant voltage, is determined by the lamp volt-amp static characteristic curve and the ballast resistance load line at the applied driving pulse voltage (V_s) value (see Fig. II-1 and Ref. 4). The lamp current and voltage pulses are rectangular in shape. In Fig. 8b, it is shown that as the cable length of R_b is increased, an exponential rise in voltage is evident. The dynamic breakdown of the lamp occurs at the point where the rising voltage waveform terminates and a sharp fall in lamp voltage is experienced. It is, in general, evident that as the $\Delta C\ R_b$ time constant becomes larger, the delay time becomes larger, but the dynamic breakdown voltage becomes smaller in value. In addition, the voltage across the lamp and cable, at pulse termination and extinguishment of the lamp, cannot suddenly disappear. The charge has to decay between driving pulses through any form of shunt conductance offered the line ΔC. Since the shunt conductance in a typical cable is small, an appreciable initial condition voltage remains across the lamp at the inception of the next driving pulse. This can be desirable, particularly in reducing the lamp starting delay time. It is noted that the initial condition voltage increases in amplitude as the line length is increased. Figures 8a, b, and c illustrate typical voltage waveforms encountered at PRR of 10 Hz with a 500-μsec duration driving pulse. Figure 8d shows a 350-μsec delay in lamp starting for a driving pulse that is only 500 μsec in duration. Figure 8d, in general, is not desirable. Although the lamp ionizes reliably, the current delivered to the lamp is limited in duration to 150 μsec.

Figure 8 illustrates the drop in voltage across a lamp as it transfers from its dynamic breakdown voltage to its maintaining voltage. The lamp is essentially parallel coupled to a charged equivalent capacitance that will not permit any sudden change in voltage across its terminals. In order for the lamp to adjust to its maintaining voltage (i. e., the intercept of the lamp volt-amp static curve and the ballast resistance load

line, Fig. II-1), the lamp must pass a pulse of current from this charged capacitance. The intrinsic resistance of the lamp can drop to a low value to accommodate the current pulse, and the operating point of the lamp can extend far into the abnormal glow region. Such operation can significantly shorten the life of the lamp. Photographs of lamp current versus lamp voltage clearly illustrate that current spikes can occur when breakdown takes place.

The peak value of the breakdown current spike becomes larger as the dynamic breakdown voltage becomes larger, i. e., fast turn of the lamp with resultant larger ΔV between breakdown and maintaining voltage. Note, however, for very short cables $\Delta C \rightarrow 0$, and the current peak begins to drop. Figure 9 illustrates the relative amplitudes of the current spike for variations in the lamp starting delay time. Peak currents in excess of 300 ma have been measured. The current spike is evident in all photographs where the lamp resistance alone must limit the line capacitance discharge current. Figure 10 illustrates how the lamp intensity follows the lamp current during the spike.

2.6 UNDESIRABLE LAMP IONIZATION MODES

Certain simplifying assumptions were made in deriving Eq. (32) for t_D, the time delay in lamp ionization. It becomes necessary to consider what can result when these assumptions are not valid.

It was assumed that $t_D < t_p$, where t_p is the pulse duration time of V_s. It can be seen from Fig. 6 that lamp ionization can still occur at a time later than t_p even though $V_L(t) < V_b$ at t_p. This is possible since the ionization curve of the lamp plots many values of V_b versus time, and if the potential across the lamp at the end of the time t_p is less than that required value of V_b at t_p, but greater than a subsequent value of V_b required at a later time on the curve, then the lamp will ionize at the later time. Note that charge retention by a sizeable line capacitance will maintain a practically constant V_{ic}.

The waveform, as displayed on the oscilloscope, will indicate the residual voltage across the lamp after V_s pulse termination. Figure 11 illustrates the situation where the lamp ionizes 300 μsec after the termination of the V_s pulse.

Careful observation of the lamp voltage waveform is necessary to establish precisely what is happening and when the lamp does ionize. It is important to note that in any event, the delayed mode of operation is

undesirable since the lamp current time pulse varies widely and in the worst case is determined largely by the charge $\Delta Q = C\Delta V$ discharged from the line through the lamp. In the delayed mode, C as a function of line length and ΔV ($\Delta V = V_b - V_m$) predominantly determine the density of the film mark. Also, ΔV becomes smaller as V_b drops in value, and the lamp current $\left(i(t) = C\frac{\Delta V}{\Delta t}\right)$ is further modified by the effective resistance of the ionized neon lamp, a nonlinear quantity.

It should be emphasized that where pulse duration times (t_p) of less than 25 μsec are employed, the delayed ionization mode is particularly prone to appear. This is because of the large increase in the dynamic breakdown voltage (V_b) required for rapid ionization of the lamp; aged lamps intensify the problem. Equal consideration should be given the fact that it is not sufficient that the lamp will ionize before the terminal point of t_p. The film-mark density is a function of exposure (see Section IV) which is directly related to the area under the lamp current time plot, and the lamp current does not start until ionization is accomplished.

2.7 EXTREME CASES OF DELAY IN LAMP IONIZATION

Consider the case where the voltage $V_L(t)$ across the lamp does not reach the lowest value of breakdown voltage along the ionization curve before input pulse termination. The line may retain much of its charge during the time interval between pulses, and this voltage becomes the initial condition voltage for the next pulse. The lamp did not ionize during the first pulse but will ionize during the second pulse. Figure 12 shows this condition; the pulse repetition rate is 100 Hz, but the lamp ionizes at a 50-Hz rate. This could be termed pulse rate division and is difficult to detect other than through waveform analysis with an oscilloscope. In extreme cases, many pulses may be required to ionize the lamp once.

Factors that can contribute to the delayed mode of lamp operation are: (1) large time constants, ΔCR_b; (2) low values of V_s; (3) short drive pulse durations, t_p; and (4) conductance paths shunting the lamp. Conductance paths can be created by damaged cables, aging effects, moisture, etc.

The presence of a shunt conductance across the lamp, $G_p = \frac{1}{R_p}$ can limit $V_L(t)$ in the steady state to $V_s \frac{R_p}{R_p + R_b}$. Thus, if $R_p = R_b$,

$V_L(t)$ will be limited to a maximum value of $V_s/2$. This, of course, can cause the lamp to fail to ionize. The R_p should be at least 10 R_b, preferably 2 megohms or larger.

The presence of an open-circuited or shorted cable is easily determined by observing the waveform. For the shorted cable, no voltage appears across the line, V_s, being totally dropped across R_b. For the open-circuit cable, the waveform will appear as a series of sawtooth waveforms. The rising portion is described by the ΔCR_b time constant. If R_p is sufficiently small, then the time constant is modified to be $\Delta C \frac{R_p R_s}{R_p + R_s}$. The falling portion of the waveform is dictated by the ΔCR_p time constant. The pulse repetition rate (PRR) enters in determining the average DC level across the line, and the sawtooth is observed to run at the same frequency as PRR.

One additionally observed phenomena is mentioned relative to large ΔCR_b installations. Some lamps apparently transcend to the arc state during the passage of the current spike and subsequent to this event cannot be maintained in the ionized state by the current permitted by the R_b ballast resistance. Thus, immediately following breakdown and the current spike passage, the lamp "goes out". The V_L across the lamp will drop to a nominal 20 volts and must again rise as dictated by the ΔCR_b time constant until the lamp will again ionize. It is observed, however, that the second ionization breakdown is accomplished at a substantially lower voltage (assumed because of a high residual charge carrier density) than the first breakdown. This "double starting" of the lamp produces two distinct and separate light pulses.

2.8 IMPROVEMENT OF PULSE TRANSMISSION THROUGH LENGTHY CABLES

The technique of driving a lamp in the manner elaborated on in Section 2.6 has two things in its favor (1) simplicity of installation and (2) means of observing lamp performance from a remote location. In situations where the lamp must be driven through a long transmission line, certain techniques can reduce the lamp ionization delay.

2.8.1 Split Ballast Resistor

Consider the case where a part of the lamp ballast is located remotely at the camera and a minimum amount is retained within the generator for short-circuit protection. The ΔCR_b time constant has

been reduced to an appreciably smaller value with reduction in R_b. The voltage rise across the lamp corresponds to this smaller time constant. At lamp starting, the remote ballast aids in limiting the current spike from the line ΔC. The combined remote and local ballast resistance limits the lamp maintaining current at the desired lower value.

Examination of the voltage and current waveforms for a lamp driven in this manner does indicate that appreciable reduction in ionization delay can be achieved. In general, the lamp will now ionize at a higher dynamic breakdown voltage. Examination of the current waveform leading edge reveals in many cases the total absence of a current spike for split ballasts in the order of 30 KΩ. Added problems are now apparent, however: (1) The ionization of the lamp can no longer be detected by waveform observation at the generator, and (2) at driving pulse termination, the lamp current, for lengthy cables, shows an extended fall time. However, the remote ballast resistance can be replaced by a "dynamic ballast"; a constant current regulating transistor at the lamp and the current waveform would show considerable improvement. The current regulating transistor would remain saturated initially until the lamp breakdown occurred and the potential across the lamp and "dynamic ballast" were large enough to supply the desired current. At pulse termination, the transistor would again saturate in an effort to maintain the regulated current level, thus quickly discharging the line.

2.8.2 Transmission of the Timing Pulse with Proper Cable Termination

If the source and load impedance were matched to the cable characteristic impedance, Z_o, then minimum delay would result in pulse transmission. This approach has been employed by removing the high voltage switching transistor, power supply, and ballast resistance from the generator and placing them at the camera position (Ref. 5) as shown in Fig. 13.

In Fig. 13 it can be seen that a 2-volt pulse is adequate to gate the remote high voltage switching transistor so that moderate voltages and current levels are transmitted along the transmission line. For best results, the switching transistor should be as close as possible to the lamp. Battery supplies may be used to power the lamp and a "keep alive" source will aid materially in reducing lamp "turn on time". The keep alive circuit serves to maintain the lamp in a constant state of low level ionization. Lamp delays of less than 5 μsec can be achieved easily, even at low current levels and low pulse repetition rates. Resistor R is used to bypass the transistor I_{cex} around the lamp and permit closer control of lamp keep alive current level. A slightly different configuration could permit combining the 300-volt battery and the keep alive

source into one. Although the use of a circuit such as Fig. 13 will produce a minimum of lamp starting delay and yield well-defined current pulses, it does possess certain disadvantages in a multiple-camera installation.

For best results, separate switching transistors must be used at each camera. Remote monitoring of lamp voltage waveforms is not possible. The status of battery supplies is difficult to assess, and the installation complexity increases. In certain installations, a possibility not to be overlooked is the use of the circuit in Fig. 13 in a "service package" located as close as feasible to several cameras with fan out to the cameras from the one switching transistor and power supply.

2.8.3 Effect of Keep Alive in Reduction of Lamp Ionization Delay

If a potential source could ionize the lamp and maintain a low level current through the lamp between timing pulses, then at the timing pulse the potential swing required to bring the lamp from a low to a high brightness state should be considerably smaller than the dynamic breakdown voltage required of a nonionized lamp. Correspondingly, the time delay should be reduced in the presence of line capacitance since the capacitance charge fluctuation would be appreciably lessened. Further, the lamp would not be required to pass a current spike when starting. Figure 14 indicates this to be true.

Figure 14 shows voltage and current waveforms for a lamp driven at 100 Hz, with and without keep alive. The time constant of this circuit was about 300 μsec, so that the voltage across the lamp with an initial condition of 30 volts had reached 100 volts in 60 μsec, at which point the lamp ionized as indicated by the current trace and break in voltage waveform. Thus, a 60-μsec delay in lamp starting (from the time of application of driving pulse) is experienced. With keep alive, the lamp is preionized and operating at a small ($<$100-μa) current level. The initial condition is nominally 55 volts. The arrival of the timed 375-volt driving pulse starts to shift the lamp operating point to a higher maintaining voltage of approximately 72 volts. A detectable increase in lamp current can be seen in some 10 μsec with the full 6-ma level achieved in 30 μsec, or one-half the time required without keep alive. Note the absence of the current spike and the lack of overshoot in the voltage waveform. The delayed rise in lamp current follows the delayed rise in $V_L(t)$ because of the ΔCR_b time constant.

It is difficult to define the condition of the lamp (on or off) at the termination of a driving pulse. The current level during the pulse, the

ion recombination rate, the impedance through which the residual charge on the "line capacitance" must discharge, the switching from the drive pulse voltage to a lower keep alive voltage (diode switching) with a much larger ballast resistance (1.5 megohms), all contribute in defining the voltage waveform between pulses as shown in Fig. 15 (lower trace). The top trace displays the current pulse through the lamp during the timed voltage driving pulse. There is no evidence of detectable current between pulses, but this is expected as the pulses are 20 ma, and the keep alive current should be less than 100 μa.

A factor that precludes the use of keep alive at the lower pulse repetition rates, where the greatest benefit in minimizing lamp starting delay is to be derived, is shown in Fig. 16. Here, an NE51H is being driven at a 10-Hz PRR. The top trace, lamp voltage, discloses relaxation oscillation at some 300-Hz rate. The lower trace indicates spikes of current through the lamp. It has been observed that the spikes can, under certain conditions of camera film speed and slit dimensions, cause undesirable marking of film.

The tendency of the circuit to oscillate is a function of the line capacitance, the applied voltage magnitude, and the intersection of the ballast resistance load line in the negative resistance region of the lamp characteristic curve. Elimination of capacitance (match impedance of cable or use a very short cable) would stop the oscillations. Reduction of the ballast resistance to a value to keep the lamp in a stable region would also eliminate the problem. The stable current value, however, becomes objectionably large. A complete coverage of the neon lamp as a relaxation oscillator is given in Ref. 4.

2.8.4 Comparison of the NE51 and NE51H Neon Lamps

In the case where large ΔCR_b time constants (greater than 200 μsec) are involved and low lamp currents (i. e., low lamp intensity at slow film speeds) are desired, NE51 is preferred over NE51H (Ref. 6) because of the substantially lower static breakdown voltage value for NE51. Manufacturers rate NE51 and NE51H at 90 and 135 volts, respectively. The slope of the ionization curves for time periods greater than 100 μsec is quite low (see Fig. 6). The reduction in lamp starting delay then becomes a function of the time difference required for $V_L(t)$ to change by this nominal 45 volts. Figure 17 illustrates this reduction in lamp starting delay for a large time constant (more than 500 μsec). Five lamp voltage waveforms are shown; three waveforms with NE51H lamps and two waveforms with NE51 lamps are illustrated. It is noted that the NE51 lamps break down at a nominal 80 volts, and the NE51H lamps break down between 125 and 150 volts. The time reduction

offered by the NE51 lamps is clearly evident. However, the NE51 lamps age rapidly with increasing breakdown voltage values and blacken when driven at high (20- to 30-ma) current levels (see curves F and G, Fig. 6). It has further been observed that little difference exists in the breakdown voltages of the two lamps when used with low time constant (10-μsec) circuits; in fact, the NE51 begins to ionize erratically when driven by fast rise voltage pulses.

In summary, it may be stated that the neon lamp performs satisfactorily for marking motion-picture film when certain problems such as lengthy transmission lines, aging characteristics of the lamp, and short driving pulses are not experienced. A means of visual waveform analysis of system operation is most desirable.

To illustrate what can be done to reduce lamp ionization delay, a worst case condition was selected. An NE51H lamp was driven through 350 ft of RG62 cable at a 6-ma current level (which requires a 51-KΩ ballast resistor, ΔCR_b = 0.0045 μf x 51 KΩ) in a conventional manner as shown in Fig. 18a. The lamp ionization delay was found to be 135 μsec with the lamp breakdown voltage at 175 volts. Recall that a low PRR and low lamp current (large R_b) are two major contributors to a long delay time. Next, the R_b was removed from the generator and replaced by a "dynamic ballast resistor" as shown in Fig. 18b. This circuit constitutes a current regulator with Q_4 collector current controlled by $E_z/R7$ (ignoring V_{bef}, Q_4). The R_7 was chosen to deliver a 6-ma current to the lamp. The second departure from the conventional approach was to modify the portion of the circuit containing Q_3 such that it would be current limited at 300 ma. With reference to Fig. 18b, when $V_2 + V_{bef}$, $Q_3 = V_1$, Q_4 acts as a current regulator with the voltage drop across R_6 determined by the value of V_1 applied to Q_3 (with respect to ground reference). Lower levels of current through Q_3 will not prevent saturation of Q_3; that is, Q_3 will act as a closed switch. The object is to permit Q_3 to pass a large pulse of current, not to exceed 300 ma, at the beginning of the voltage drive pulse such that the lamp will experience a fast rise time voltage across its terminals. This circuit was assembled in breadboard form, and tests were made with the NE51H lamp. It was found that the voltage at the terminal end of the 350-ft cable had reached 375 volts in 7 μsec. The inrush current at the sending end of the transmission line exhibits a current pulse 7 μsec in duration with an initial amplitude of 300 ma and a terminal amplitude of 250 ma. The lamp ionized within a nominal 10 μsec after V_s pulse initiation. The lamp current pulse leading edge was evident at this time, attaining a steady current level of 6 ma within 0.4 μsec after the start of lamp ionization. Figure 18d (taken from oscilloscope traces) compares

the current pulses obtained with the circuits shown in Figs. 18a and b. The 130-μsec delay compared to the 10-μsec delay is clearly evident, and the superiority of the circuit shown in Fig. 18b is obvious. The decay in lamp current at pulse termination indicates the same rate for both traces.

Several different lamps were used in the circuit of Fig. 18b, and it was observed that lamp ionization was accomplished over the range from 5 to 30 μsec. Some lamps would ionize before the full 375 volts would appear across the lamp, others would fire erratically with delay time variance from pulse to pulse.

The pulse duration time across a sample stable lamp (with a 5-μsec delay) was reduced to 50 μsec (the limit of the pulse generator at the low pulse repetition rate). The lamp continued to exhibit a stable current pulse for 90 percent of the drive pulse duration.

The circuit in Fig. 18b offers a brute force approach to fast pulse transmittal through the line. The large surge current experienced at pulse initiation represents something of a problem in terms of the generator power supply (375 volts) and the switching transistor Q_3, when multiple timing lamps must be driven. High voltage silicon transistors in the class with Q_3 are available and capable of switching several amps of current; the supply must offer low inductance, high pulse current capabilities.

The dynamic ballast current regulator (Q_4) permits a far more precise control of lamp current than the R_b approach used in Fig. 18a. Transistor Q_4 will maintain the current at the present value regardless of the maintaining voltage variations among different lamps. It is only required that the new V_L voltage be sufficiently larger than the maintaining voltage to keep Q_4 out of saturation. A noteworthy feature of this device is that R_7 can be a potentiometer, thus permitting a means of selecting a wide range of lamp currents. The variable R_7 may even be calibrated directly in terms of lamp current.

Now that a fast rise $V_L(t)$ has been achieved at the lamp, it may be noted that the erratic ionization of some lamps still possesses a major obstacle to reliable film marking. A lamp selection program may be usefully employed. Lamp stabilization by preaging may be found useful (Ref. 7); it is important in this event to note that the lamp may be polarized (see Appendix II).

The lamps can be checked within the camera by waveform examination since the erratic firing lamp can easily be detected. An approximate

indication of the lamp "age" may also be determined by the lamp maintaining voltage magnitude as viewed on the scope (see Fig. 6, curves F versus G and Fig. II-1).

For those installations where direct viewing of the voltage waveforms across the lamp cannot be made, an alternate technique of employing an integrated photodiode (Fig. 18c) (within the timing lamp block to view the lamp) can be employed when the complexity of the added wiring can be tolerated. An added advantage gained with the photodiode is that the radiated light as a function of the current pulse may be directly viewed, so that for a known driving pulse duration the lamp ionization delay can be easily determined from the scope presentation.

Figure 18c suggests a method of incorporating a keep alive source at the camera. The D_2, D_3 diode "OR" gate permits the lamp current transition from the nominal 100-μa keep alive level to the high current timed pulse level. The gate further isolates the lamp from the transmission line (minimum capacitance across lamp) so that relaxation oscillation (see Fig. 16) does not occur. A reliable keep alive circuit has been proved capable of stabilizing erratic lamps. The keep alive supply may be battery powered since the current drain by the lamp and photodiode is in the low microamp region. Lamp dark effect can be reduced by extended operation of the lamp on keep alive before a test. With the lamp preionized, the V_s driving pulse supply may be substantially reduced. A 200-volt supply is considered adequate for non-aged lamps. The lamp current time pulse performance may be monitored remotely by oscilloscope, counter, or direct oscillograph recording if desired. It should be noted that D_2 must be a high quality, low inverse leakage silicon diode.

2.9 SEMICONDUCTOR LAMP

The troublesome areas of operation of the neon lamp as a film-marking device, particularly where long transmission lines are required, prompted a search for a device that would be more reliable. Solid-state light emitting diodes (LED) were, therefore, investigated for this application. The LED device offers certain highly desirable characteristics. The device operates at low voltages, compatible with transistor circuitry and impedance levels that make matching to the transmission line practical. Thus, well-defined current pulses of short duration can readily be achieved.

Initially, experiments were performed on a silicon carbide crystal lamp. The lamp responded well to pulse application through transmission lines and possessed a linear relationship between applied current and light output, but the particular unit used did not deliver adequate light (80 ft lamberts at 100 ma) for film marking. Additionally, the rated brightness rise and fall time of less than 100 μsec did not appear adequate. However, Kerr (Ref. 6) has successfully time-marked black and white film at frame rates up to 600 frames/sec and 1-kHz PRR using a silicon carbide crystal lamp. Experiments were then conducted using a gallium arsenide phosphide diode. Some of the pertinent specifications of this diode are:

Light turn-on and turn-off time, 10 nsec, typical
Wavelength range, 6000 to 7000 angstroms
Forward current, continuous, 100 ma
Brightness at 150 ma, 1000 ft lamberts
Driving voltage at 100 ma, 1.8 volts
Peak forward current (1-μsec pulse, 300 PPS) 3-amp maximum

Since the light emitting diode forward conduction characteristics are approximately the same as a conventional PN junction diode, a large change in forward current results for a small change in forward voltage. The diode conducts at a forward voltage of 1.4 volts and increases to a forward drop of 1.8 volts at 100 ma. The driver circuit employed is shown in Fig. 19.

The R_1, R_2, and R_3 are chosen so that $\frac{E_1 - V_{be,Q2}}{R_4}$ determines I_1 to be the minimum current available to the R_5, D_1 current divider that will produce the desired "low" light level at the diode. A similar relation using E_2 produces an I_1 for maximum diode current and "high" light level. The Q_2 acts as a current regulator and will limit current in the event of a shorted transmission line. The R_2 serves as a light intensity control, and R_5 is chosen to match the characteristic impedance of the transmission line. As shown, the line is matched at the sending end but is not matched at the receiving end. The diode appears as a nonlinear terminal resistance, nominally 53 Ω at 30-ma diode current decreasing to 18 Ω at 100-ma current. The diode also possesses junction capacitance resulting in a complex impedance term that becomes significant at frequencies beyond those used in marking film. The R_5 was empirically determined to be 85 Ω, as that value best suited to minimize multiple reflections when used with the particular RG62 cable employed in the experiment. The R_L may be employed to reduce the negative reflection coefficient prevalent at the receiving end of the transmission line.

Figure 20 illustrates typical voltage and current response waveforms to a 1- and 10-kHz driving pulse. The leading edge of the driving voltage pulse shows that initially the drive pulse looks into the nominal 93 Ω characteristic impedance of the cable. The propagation delay time, t_d, of the cable is 480 nsec; 1 μsec nominally is required for the pulse to travel to the diode and be reflected back to the input. The decline in voltage subsequent to this time is attributed to the negative reflection coefficient at the terminal end. Ideally, a shorted cable would be indicated by a total collapse of the drive pulse after the second t_d time period. Alternatively, an open-circuit cable would show the applied voltage pulse doubling in amplitude following the second t_d period. With the aid of a good oscilloscope at the sending end of the transmission line, the system becomes a form of time domain reflectometer, and the distance out along the cable that a shorted or open condition exists can reasonably well be approximated as one-half the time duration of the sending end voltage discontinuity divided by 1.6 nsec/ft (applicable to polyethylene dielectric).

Figure 20d illustrates the pulse response capabilities of LED. Here the diode is driven at a 200-kHz PRR by a pulse 0.7 μsec in duration. The specified driving pulse represents the maximum performance obtainable from the laboratory pulse generator employed during the experiments. The three traces (top to bottom) show (1) the pulse generator voltage waveform to the LED driver, (2) the light output of LED sampled by a PIN silicon photodiode, and (3) the LED current measured by a Tektronix current probe (50-MHz bandwidth). It is significant to note that the diode current and light response to the driving voltage pulse follow the voltage pulse waveform quite well. The implication then is that the frequency response limitation lies with the pulse generator (even through the t_r pulse rise time is < 50 nsec) and not with LED.

The desirable high frequency response characteristics of this type of diode are illustrated in Fig. 21. The data of Fig. 21 were recorded by photographing a spectrum analyzer display of the output of a photomultiplier tube which, in turn, was responding to LED driven by a 90-MHz sinusoidal current waveform.

The light emission of LED is small relative to the neon lamp, but a comparable surface illumination at the film plane was found between LED (at 100 ma and fitted with a lens assembly) and an NE51H high brightness lamp at a 15-ma current level. A silicon photodiode with equal spectral response to the two light sources was used in the comparison. The lens assembly employed two positive, coated, short focal length lenses.

Assuming an I^2t rating for the diode of 27×10^{-4} amps^2-sec, 200-ma, 50-μsec pulses at 1-kHz rate could safely drive the diode. Heat sinking of the diode base to the lens assembly barrel should be employed.

SECTION III
DESCRIPTION OF AN OPERATIONAL TIME-MARK GENERATOR

The circuitry used to supply the timed pulse train to the solid-state light emitting diode is the same as that employed in a 15-camera timing light generator which had previously been designed and constructed.

The circuit is completely assembled on a 3- by 6-in. printed circuit board, lacking the +5 and -1.5 volt logic power supplies. With the exception of three transistors and discrete resistor capacitor components, all circuit elements are of the integrated circuit type. The basic building blocks are dual J-K flip-flops and Quad 2 input gates. Since these are standard items employed in quantity in digital computers, the cost of materials was quite reasonable. The major expense incurred was the purchase of a tuning fork oscillator. Figure 22 shows a block diagram of the timing light generator; Fig. 23 gives the generator logic circuit in schematic form.

The 1-kHz tuning fork oscillator (0.01-percent accuracy) produces a 5-volt square wave signal which is passed through a shaper to improve the waveform rise and fall time to less than 0.1 μsec. The shaper output fans out to a 1-shot multi, and to a J-K flip-flop, decade divider. The divider produces a 100-Hz output that fans out to two 1-shot multivibrators and a second decade divider. The second divider produces a 10-Hz output which is routed to a 1-shot multivibrator. The five 1-shot multivibrators serve to produce controlled width pulses at the triggered pulse rate. Each multivibrator is equipped with a printed circuit board mounted potentiometer for pulse width adjustment.

The outputs of the 1-kHz multivibrator and one of the 100-Hz multivibrators are combined through a diode "OR" gate to produce a 1-kHz timed pulse train with a superimposed accentuated tenth marker pulse. The same approach is employed for the 100-Hz pulse train. The three pulse trains are then available for signal pickoff at the three frequency selector switches that route the desired PRR pulse to the lamp drivers. The lamp drivers would appear as the solid-state LED driver (Fig. 19) or alternatively high voltage, NPN silicon power transistors (Q_8, Fig. 23) employed to switch 375 volts to neon lamps.

The use of solid-state LED considerably simplifies the fabrication, number of components, and packaging of the timing light generator as compared to a generator for use with neon lamps.

In summary, the solid-state LED may be said to offer certain desirable features as a timing lamp. The diode current and attendant lamp intensity can be continuously varied and easily controlled without the penalty of lamp starting delays, even at frequencies well in excess of 10 kHz and regardless of reasonable transmission line length. There are no ionization problems or current spikes as encountered with neon lamps. When operated within the manufacturer's specifications, the lamp may outlast the useful life of the camera. No high voltage power supplies or keep alive sources are required. Parallel or even series operation of the diodes is a possibility.

The physical size of the diodes would permit ready application to most cameras without extensive modification. The light output of the diode is small compared to the neon lamp, but proper utilization of this light by close proximity to film or by lens collimation of the source suggests its satisfactory application. Extensive research is presently improving LED in its various forms, and its future application in the field of time-marking film appears to be quite promising.

It is interesting to note that within the few months of acquisition and experimenting with the diode reported on herein, an LED of the GAP type has been announced with a cost reduction of four to one. This diode is stated to be capable of a peak brightness greater than 10,000 ft lamberts when pulse driven at a 1-kHz PRR with 10-μsec pulse widths.

SECTION IV
TIMING LIGHT INTENSITY/FILM-MARK DENSITY RELATIONSHIP

The discussion to this point has revolved around those electrical circuit variables that influence the reliable application of the time mark to film. The residual portion of the problem is concerned with the ease of detection and the definition of the time mark. Any detailed description in this area would involve certain nomenclature relegated to the science of sensitometry and photometry.

It is considered beyond the scope of this report to enter these fields other than to extract the minimum information that may permit the assignment of a qualitative index of our mark on film.

The following section attempts to present information useful in obtaining an intuitive understanding of the factors relating the lamp current time pulse to the resultant film-mark density. The latter part of the section is devoted to the discussion of a current ramp-density wedge generator as a device useful in the direct association of lamp current pulse and time-mark density.

4.1 PHOTOGRAPHIC PROPERTIES OF FILM

Sensitometry is concerned with the description and measurement of the photographic properties of sensitized materials. The best method of presenting sensitometric data (Ref. 8) is with the characteristic curve. This is a plot of the sensitized material response, optical density, versus the logarithm of the exposure. Figure 24 shows the general form of the characteristic curve for photographic film.

The density of a silver deposit on film is normally determined with a densitometer and is defined as the logarithm of the opacity of the silver deposit:

$$\text{Density} = \text{Log Opacity} = \text{Log} \frac{1}{\text{Transmission}}$$

where (33)

$$\text{Opacity} = \frac{\text{Incident Light}}{\text{Transmitted Light}}$$

The term exposure refers to the total amount of luminous energy which acts on the photographic material.

$$\text{Exposure} = \text{Intensity of Exposure} \times \text{Time of Exposure} \tag{34}$$

The logarithm of exposure is used in plotting the characteristic curve. The two factors, intensity and time (except at very low and high levels of intensity), act independently. The slope, or gradient, at any part of the curve indicates how rapidly the density changes with changes in exposure. The slope of the linear portion of the curve is called the gamma (γ) of the film. A high gamma film (narrow exposure range) produces high contrast images, few shades of gray between black and white.

Technical data sheets for a specific film will usually show a family of characteristic curves showing gamma variations as a function of development time at a specific temperature. A concept of film "speed"

may be gained from Fig. 24. Displacement of the curve to the left or an increase in the slope of the curve represents a transition from a slow- to a high-speed film. For a given value of intensity, a shorter exposure time is required to achieve the same image density.

Spectral sensitivity curves are usually employed to show the variation in exposure required to maintain a constant density for variations in the wavelength of the incident light. It is important that the film be sensitive to the timing light radiation.

4.2 LIGHT INTENSITY

The luminous (visible) intensity of a point light source is expressed as the radiant energy (in the visible region of the spectrum) emitted per second, per unit solid angle ($d\omega$) described by:

$$\text{Luminous Intensity } I = \frac{df}{d\omega} \tag{35}$$

and

$$F = \int_0^\infty L_\lambda \, f(\lambda) \, d\lambda \tag{36}$$

where F is the total luminous flux (luminous energy per second, in watts).

L_λ = Relative luminosity at the wavelength λ, pertaining to the relative magnitude of the visual sensation produced by equal amounts of radiant energy of different wavelengths

$f(\lambda)d\lambda$ = Radiant flux in the wavelengths between λ and $\lambda + d\lambda$, where $f(\lambda)$ is given by Planck's equation for a black-body radiator

The measure of the intensity of illumination on a surface is called illuminance (E) and is the luminous flux incident on unit area of the surface. The E corresponds to intensity of film exposure. If the surface is normal to the point source, then the intensity of surface illumination (E) varies inversely as the square of the distance (r) from the source and directly as the intensity of the source.

$$E = \frac{1}{r^2} = \frac{dF}{dA} \tag{37}$$

The unit of E is the foot-candle or candle-meter (intensity of illumination from a 1-candle-power source at a distance of 1 ft or

1 meter, respectively). A unit of F is the lumen, and the illumination of a surface expressed in lumens per unit area is numerically equal to the intensity of illumination expressed in candle-meters. This is so because at 1-meter distance from the source, one steradian subtends an area of 1 meter^2. Thus, 1 candle-meter = 1 lumen/meter^2 = 1 lux.

One additional expression encountered in rating light sources is the brightness of the source. The above definition of intensity I assumed a point source of light. For an extended source (one whose dimensions are not small, compared to the distance to the illuminated surface), the brightness of the source is defined as the intensity of the source per unit area (also called luminance).

A unit of measure of brightness is the foot-lambert where 1 ft lambert = $\frac{1}{\pi}$ candles/ft^2.

4.3 DEFINITION OF A TIMING MARK

A somewhat arbitrary approach of assigning density values to timing marks has been employed. Observation of film strips on the light table for clear definition without halation resulted in the following classification:

Timing-Mark Optical Density	Comment
Less than 1	Unsatisfactory
1 to 1.5	Inferior
1.5 to 2	Marginally good
2 or larger	Very good if not accompanied by halation

The terms "flare" or "halation" are used to denote a grossly enlarged mark with film fogged over into the image frame in severe cases. The desired sharp density gradient at the time-mark leading edge has been lost.

Relative to the mark density classification and with reference to Fig. 24, it can be seen that good marks are obtained for exposure values applying to the upper shoulder of the curve.

The maximum obtainable density is greatly dependent on the film properties and the development process. Figure 24 indicates a maximum density of two corresponding to a gamma of one; however, for a

given value of exposure a film may yield a density gradient of less than one to three just in the development process. An attempt to greatly exceed the maximum exposure value given for a specific film may produce an effect known as solarization where a decrease in density is observed.

4.4 PROBLEM OF ESTABLISHING A QUALITATIVE RELATION BETWEEN TIME-MARK DENSITY AND LAMP CURRENT/TIME PULSE

It was previously stated that the light output of the neon lamp varies in direct proportion to the current through the lamp (Fig. 10 and Ref. 4). If the lamp current/time pulse product can be accurately determined, then the conversion of this product to an appropriate value of exposure as indicated by the film characteristic curve should be sufficient to predict a desired density time mark. A reliable approximation of the film plane surface illumination is complicated by such factors as the extended nature of the light source; the orientation and spacing of the electrode (and the glow region on the electrode) relative to the film and the light slit; and the variable attenuating nature of light transmission through the glass envelope of the lamp, subject to sputtered electrode deposits. In one instance (Ref. 9) a photometer has been employed to sample the effective illuminance at the film plane. The photometer response to the spectral quality, and to the pulsed nature, of the light source must influence its calibration.

Should the desired value of exposure be feasibly obtained, several effects still remain that influence the resultant time mark on film: the film will move a finite amount during a light pulse, an intense light source may produce light scattering within the emulsion, or reflection may take place from the film substrate. The effective collimation of the light beam passing through the slit within the camera can also be an influencing factor.

Variation in density can occur as a function of the development process, where the prime requisite is to optimize the event image density. Various effects associated with the photographic process such as the reciprocity effect, the Clayden effect (pertinent to the lamp current spike), the solarization effect, and the adjacency effect (accumulation of reaction products in the developer) can contribute to unpredictable results. Finally, the spectral sensitivity of the film must be matched to the spectral quality of light emitted by the source.

A simple method to permit a direct comparison between time-mark definition and density to the lamp current time pulse in the presence of other variables peculiar to a specific installation was developed.

4.5 CURRENT RAMP-DENSITY WEDGE GENERATOR

A novel technique using a controlled linear current ramp was applied to the event lamp of a test camera while timing marks were simultaneously applied to the opposite side of the film strip. The current ramp duration was so selected to permit a nominal 15 to 20 in. of film to pass through the camera during one ramp. The ramp was chopped to simulate the actual timing lamp pulse of light. The maximum value of current at the ramp peak was selected to overexpose the film and the minimum value of ramp current chosen to underexpose the film. This device is called a current ramp-density wedge generator, shown in Fig. 25. The wedge generator produces a linear current ramp for application to the film-marking lamp. Transistors Q_1 through Q_4 produce a sawtooth waveform or a linear voltage ramp. The voltage ramp time was $t = \frac{EC}{i} = \frac{ECR}{E_z}$ sec where E = the peak point voltage of Q_2; C = timing capacitor; i = Q_1 collector current; E_z = Zenner diode voltage. Note, Q_1, R, and E_z comprise a constant current regulator. The multivibrator gates the Q_5 chopper in accordance with the desired current repetition rate and driving pulse width.

With a known minimum to maximum value of current delivered per ramp, it becomes a simple matter to view the "density wedge" on the processed film and select the optimum value of lamp current to produce the desired timing-mark density. The frame rate at the time of the particular ramp can also be approximated. Since the ramp time can be accurately known, the frame rate becomes frames per ramp divided by ramp time. Of course, timing marks can also be concurrently applied to the opposite film margin while the film run is made. The ramp generator circuit shown is normally a free-running device; it will apply a continuous series of density wedges to the entire reel of film. If this is not desired, the generator can be controlled for single ramp operation. A switching transistor placed across the timing capacitors in the voltage ramp generator circuit or used to hold Q_5 cutoff (i. e., override the astable multivibrator pulse train) will inhibit free running of the generator.

The ramp generator offers a simple method of permitting step changes in exposure in terms of known step changes in lamp current for known time intervals and can be employed in existing installations. The lamp current pulses produced by the ramp generator are shown in Fig. 26. The current pulse amplitude can be seen to increase linearly.

Several film strips of both black and white and color film were exposed by the current ramp wedge generator at frame rates from 24 to

2500 frames/sec. A microdensitometer scan was made of a sample strip of film, and the result is presented in Fig. 27. The optimum lamp current was found to be between from 3.0 to 6.75 ma. For this range of lamp currents, the film marks were neither underexposed nor overexposed.

Visual examination of the current ramp produced marks on the film strip which were employed to select values of lamp current for specific film speed ranges and to aid in determination of optimum light pulse widths.

Run No.	Film Type	Film Speed, frames/sec	Ramp Current, ma	Ramp Time, msec
1	Sup-4 (B&W)	1000	0 to 15	100
2	2479 (B&W)	1000	0 to 15	50
3	7258 (color)	1000	0 to 22	50
4	Super 4 (B&W)	200	0 to 15	50
5	7258 (color)	200	0 to 15	500

A Fairchild HS401 camera with an NE51H lamp was used in the above runs. It can be seen from the density plot that the entire range of lamp current would produce a visible timing mark. The region of optimum marking (minimum flare or halation, yet easily visible marks) appeared to be between 20 and 40 percent of the maximum ramp current. The spectral character of the neon lamp is such that the majority of emitted light is in the yellow-red (5700 to 7500 Å) portion of the spectrum. Thus, the low density value for Fig. 27 applied primarily to the film emulsion layer which is sensitive to red light, with the blue and green layers affected very little.

Observation of timing marks made by different types of cameras indicates that if better light collimation were employed in all cameras, a larger exposure value could be permitted without detrimental side effects. This would allow for a greater latitude in the current range used to mark the film. Figure 28 illustrates four examples of timing marks.

Figure 28a shows gross overexposure and halation. Figure 28b illustrates timing and event marks made with a camera equipped with a light collimating lens assembly and precision slit. Figures 28c and d compare marks made by the same type of camera under the same conditions of film type and speed, where the camera in Fig. 28d was equipped with a collimating device, developed by G. Martin, ARO, Inc., whereas in Fig. 28c no collimating device was used. Examination of samples (Figs. 28b and d) on a light table reveals good definition of timing mark edges as opposed to samples shown in Fig. 28a or c.

Extensive work has been performed by others (Refs. 3, 4, 6, and 10) in this area, and the conclusion reached was that where critical evaluation of time on film (i. e., examination of a film strip time mark magnified on a film reader) is to be performed, a collimated light beam is most desirable.

SECTION V
SUMMARY OF RESULTS AND CONCLUSIONS

The timing mark as applied to film in high-speed motion analysis cameras provides a lapsed time reference for the test event in progress. Successful placement of the timing mark in field installations, such as the multicamera equipped test cells at AEDC, requires an awareness of the system parameters involved. The failure to obtain a satisfactory time reference in a nonrepeatable test can represent a serious and irrecoverable loss of data. This report has attempted to present some new insight into old problems and summarize methods that may be applied to enhance the reliable acquisition of timing marks.

The timing-mark density and definition has been shown to be a function of a number of contributing factors. The current ramp density wedge generator has been proposed as a means of determining the optimum values of timing lamp intensity and pulse width for a specific camera type, film type, frame rate, and development time. The lamp intensity-pulse width product primarily determines the exposure value received by the film.

Optimum density timing marks can only be obtained when control is exercised on the lamp current time pulse product; the neon lamp as a timed light source does not easily permit this control. When the timed driving pulse is applied to the lamp through a lengthy transmission line, both the current amplitude and time duration are adversely affected. The factors contributing to this undesirable situation have been discussed at length in the early part of this report. There, a method of waveform analysis of an installation was presented, extending to those areas where timing-mark "dropout" would be experienced. Within limits, the neon lamp was shown to be satisfactory for time-marking film. To work beyond these limits, primarily large ΔCR_B time constants, other techniques (such as shown in Figs. 13 and 18c) must be employed at the cost of increased complexity of an installation.

A promising approach that permits a return to a less complex installation and produces precision current pulses beyond the capability of the neon lamp is the employment of LED as a film time-marking device.

Section III presents a discussion of the application of integrated circuit components for the generation of timed-pulse logic trains. These devices are compatible with LED and offer a practical means of extending the time-marking concept to parallel or serial BCD time codes on film. The integrated circuit concept offers the advantages of increased sophistication with good reliability at reduced cost and compact design.

In conclusion it may be stated that satisfactory time marking of film can be consistently obtained if a suitable camera installation pretest checkout procedure is employed and design consideration is given to problem areas during an installation layout.

REFERENCES

1. Goldman, Stanford. Transformation Calculus and Electrical Transients. Prentice-Hall, Inc., New York, 1955.
2. Millman, J. and Taub, H. Pulse, Digital, and Switching Waveforms. McGraw-Hill Company, New York, 1965.
3. Ferree, M. "Glow Lamps for High-Speed Camera Timing." Journal of the Society of Motion Picture and Television Engineers, Vol. 61, December 1953, pp. 742-748.
4. General Electric Glow Lamp Manual (Second Edition). General Electric Company, Nela Park, Cleveland, Ohio.
5. Boy de la Tour, R. "Accurate Coded Timing-Light Generator." Journal of the Society of Motion Picture and Television Engineers, Vol. 74, April 1965, pp. 328-331.
6. Kerr, M. A. "Miniature Light Sources for Timing Signal Recording." Journal of the Society of Motion Picture and Television Engineers, Vol. 77, March 1968, pp. 210-214.
7. Johnson, J. H. "Improved Camera Timing System Techniques." Report No. TOR-169 (3301-02)-1 (AD461386), June 1963.
8. "Kodak Plates and Film for Science and Industry." Kodak Scientific and Technical Data Book (First Edition). Eastman Kodak Company, Rochester, New York, 1967.
9. Dearing, L. M. and Hiller, R. E. "A Photometer for Measuring the Output of Timing Lights." Journal of the Society of Motion Picture and Television Engineers, Vol. 75, November 1966, pp. 1092-1094.

10. Hiller, R. E. and Dearing, L. M. "Camera Timing Marker with Dual Spark and Neon Light Sources." Journal of the Society of Motion Picture and Television Engineers, Vol. 74, October 1965, pp. 897-900.

11. Dougherty, C. R. and Smith, R. D. "Measuring the Delay Time of Glow Lamps." Electronic Design. March 30, 1964.

APPENDIXES

I. ILLUSTRATIONS

II. NEON GLOW LAMP CHARACTERISTICS

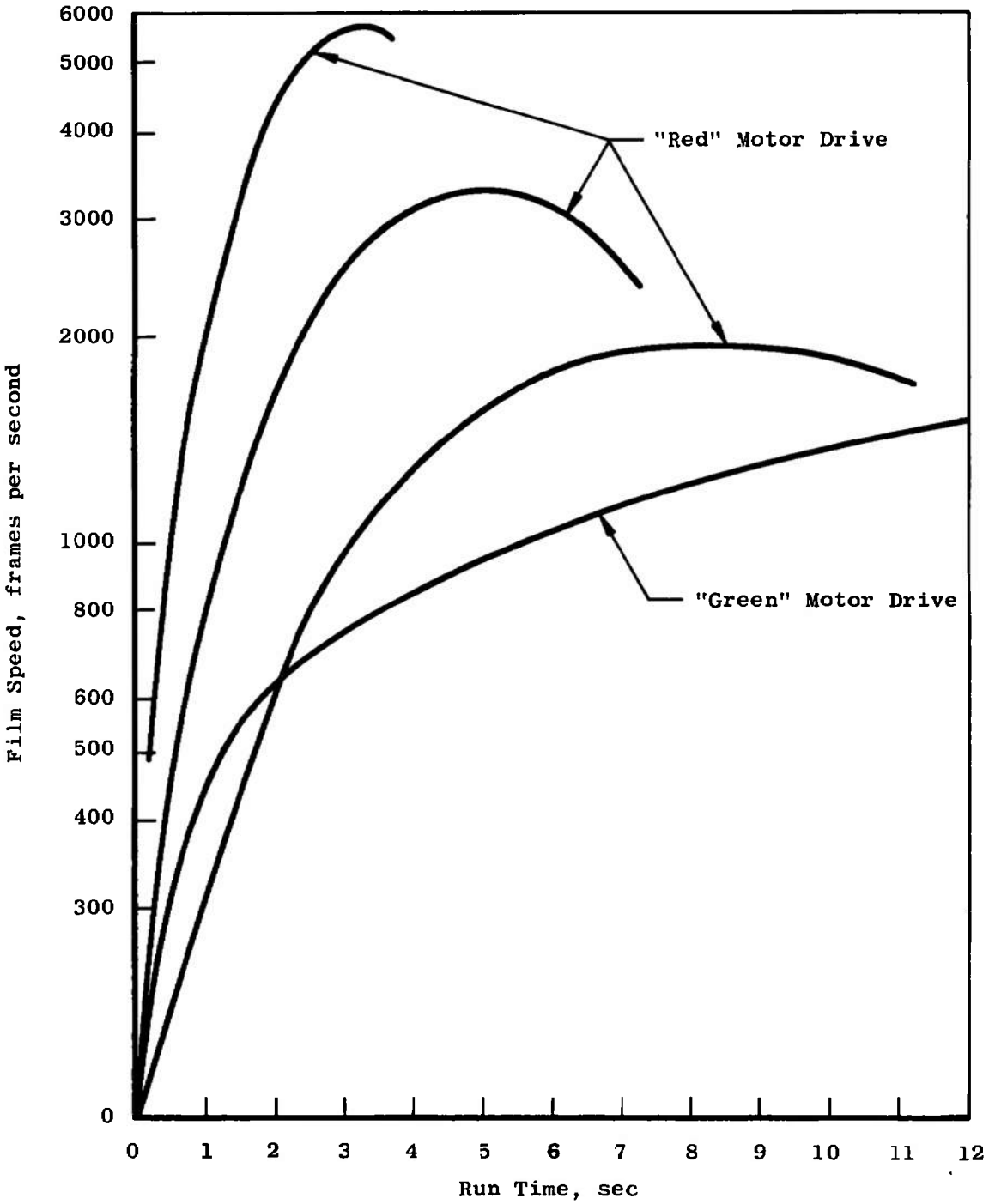

Fig. 1 Speed-Time Characteristics of a High-Speed Camera (400 ft of Supply Film)

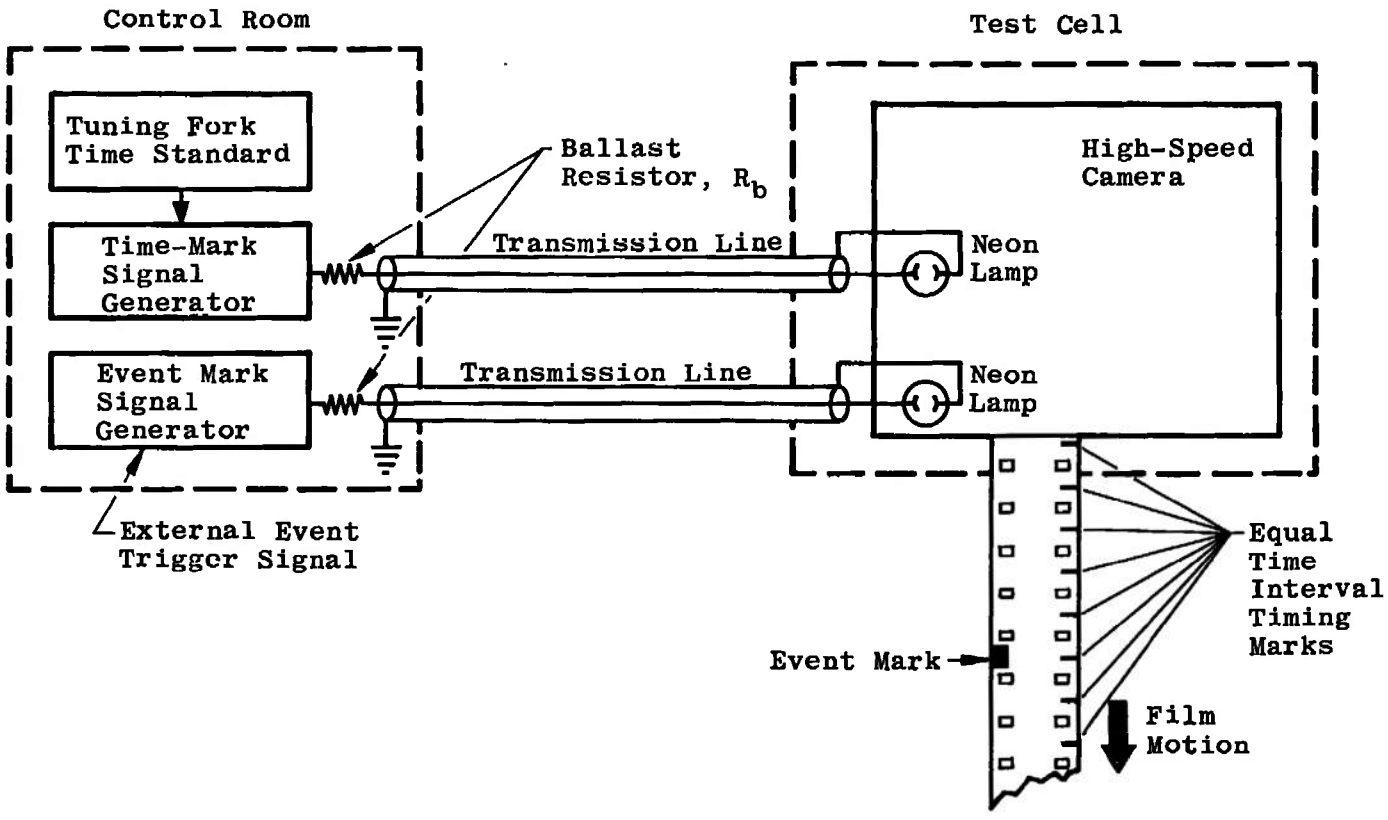

Fig. 2 High-Speed Camera Time and Event Signal Generator

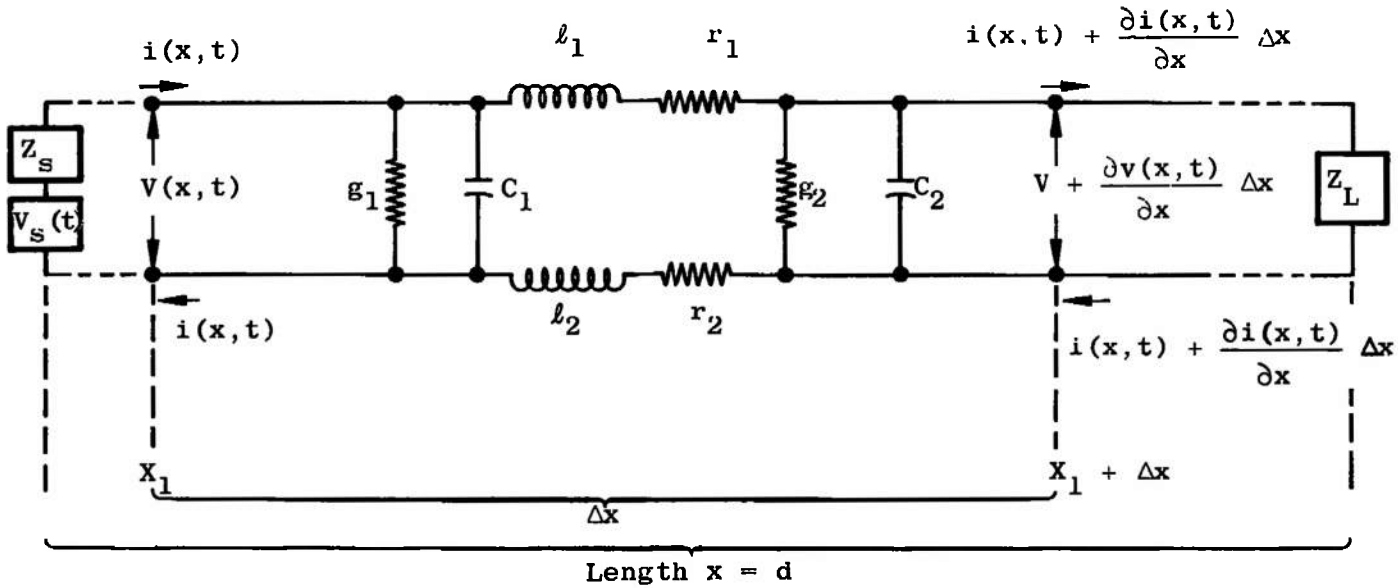

$R\Delta x = r_1 + r_2$ = Resistance per Δx Length of Line

$L\Delta x = \ell_1 + \ell_2$ = Inductance per Δx Length of Line

$C\Delta x = C_1 + C_2$ = Capacitance per Δx Length of Line

$G\Delta x = g_1 + g_2$ = Leakage Conductance per Δx Length of Line

$V_s(t)$ = Signal Generator Time Function Voltage

Z_s = Signal Generator Output Impedance

Z_L = Load Impedance

i(x,t) = Inverse Laplace Transform of I(x,s), the Current at Any Point along the Line

V(x,t) = Inverse Laplace Transform of V(x,s), the Voltage at Any Point along the Line

Fig. 3 Analytical Model of a Transmission Line

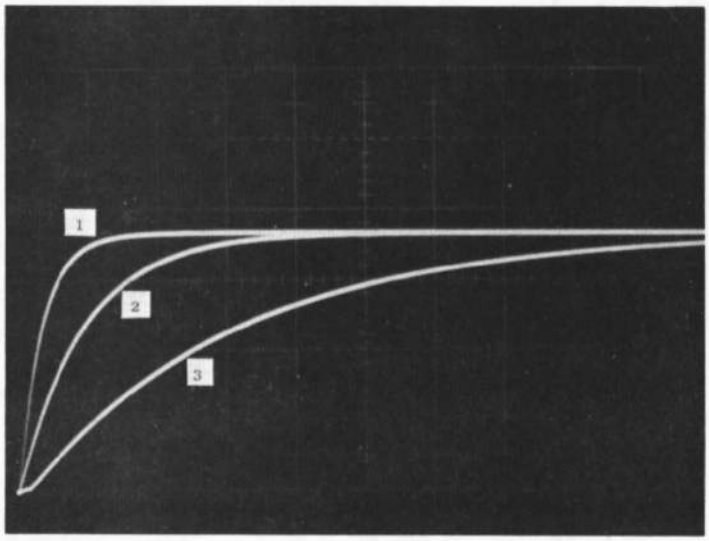

Horizontal Scale,
50 μsec/cm

Vertical Scale,
100 volts/cm

Transmission Line Conditions

1. 400-ft-long RG58U Transmission Line, $\Delta C \approx 0.012$ μf, $Z_o = 50$ ohms
2. Output Terminal Open Circuited
3. $V_s(t)$ Rise Time, 1 μsec
4. Trace 1, $R_b = 1.2K$, $\tau = 15$ μsec
   Trace 2, $R_b = 3.8K$, $\tau = 45$ μsec
   Trace 3, $R_b = 12.5K$, $\tau = 150$ μsec

Fig. 4 Open-Circuited Transmission Line Output Voltage Waveforms

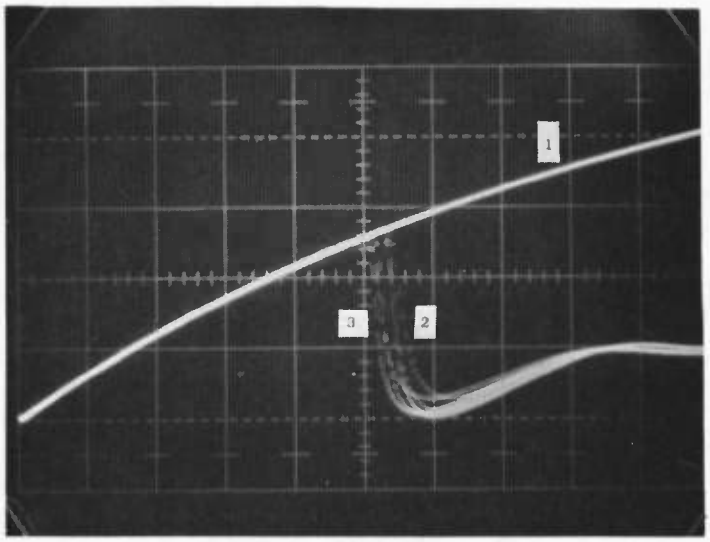

Horizontal Scale,
20 μsec/cm

Vertical Scale,
50 volts/cm

Transmission Line Conditions

1. 400-ft-long RG58U Transmission Line, $\Delta C = 0.012$ μf, $Z_o = 50$ ohms

2. $V_s(t)$ Rise Time, 1 μsec

3. Trace 1, Output Open Circuit

   Trace 2, Output Terminated with Neon Lamp

   Trace 3, Transmission Line Replaced by 0.012-μf Capacitor in Parallel with a Neon Lamp

Fig. 5 Neon Lamp Driving Voltage Waveforms

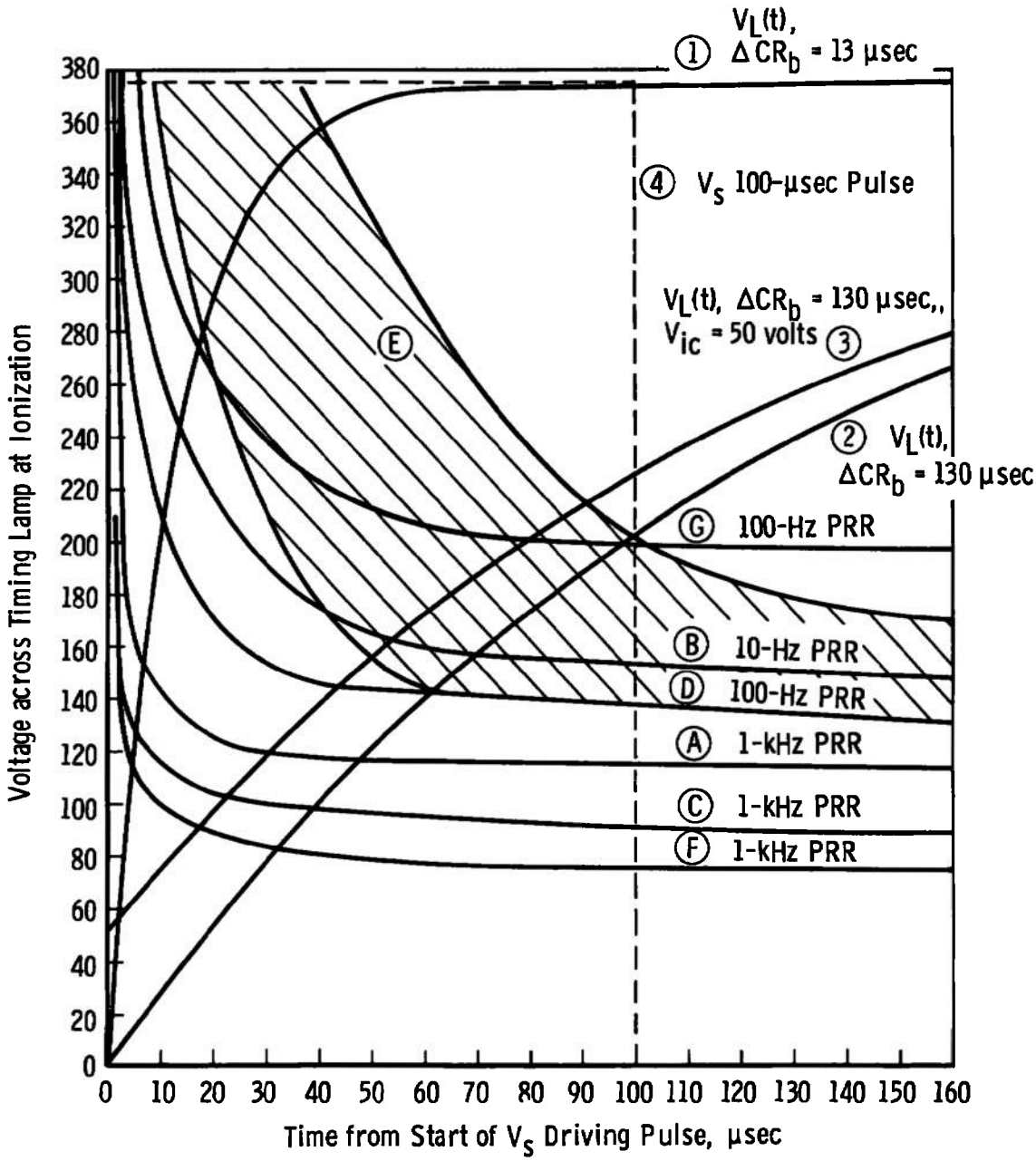

Fig. 6 Neon Lamp Ionization Curves in Time Comparison with Three Representative V_L Waveforms

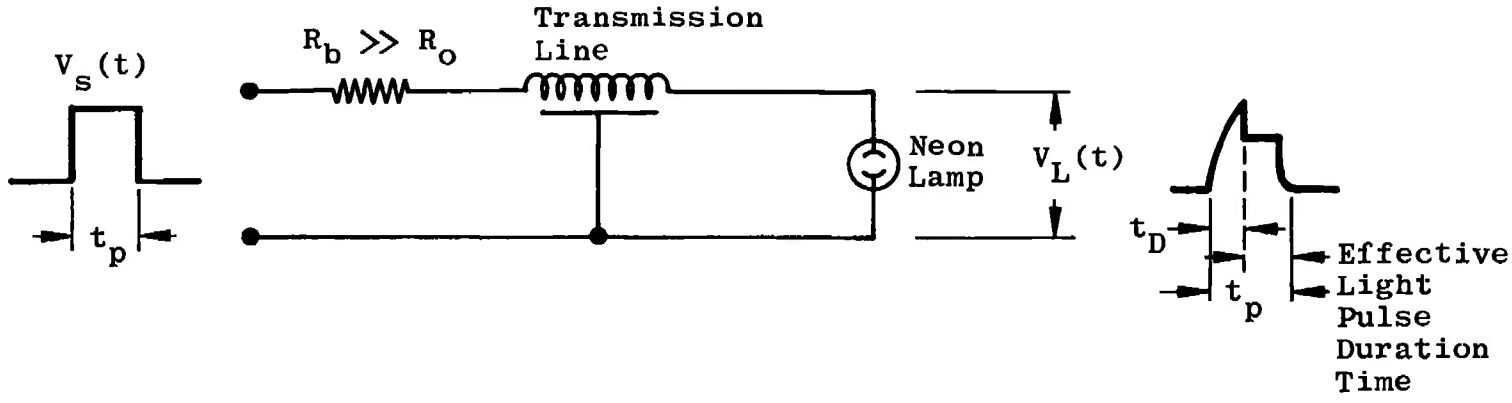

a. Timing Lamp Installation Model

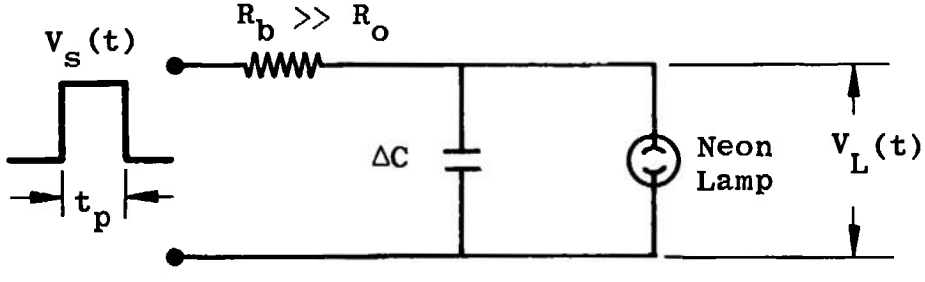

b. Timing Lamp Installation Equivalent Circuit

Fig. 7 Timing Lamp Installation Model and Equivalent Circuit

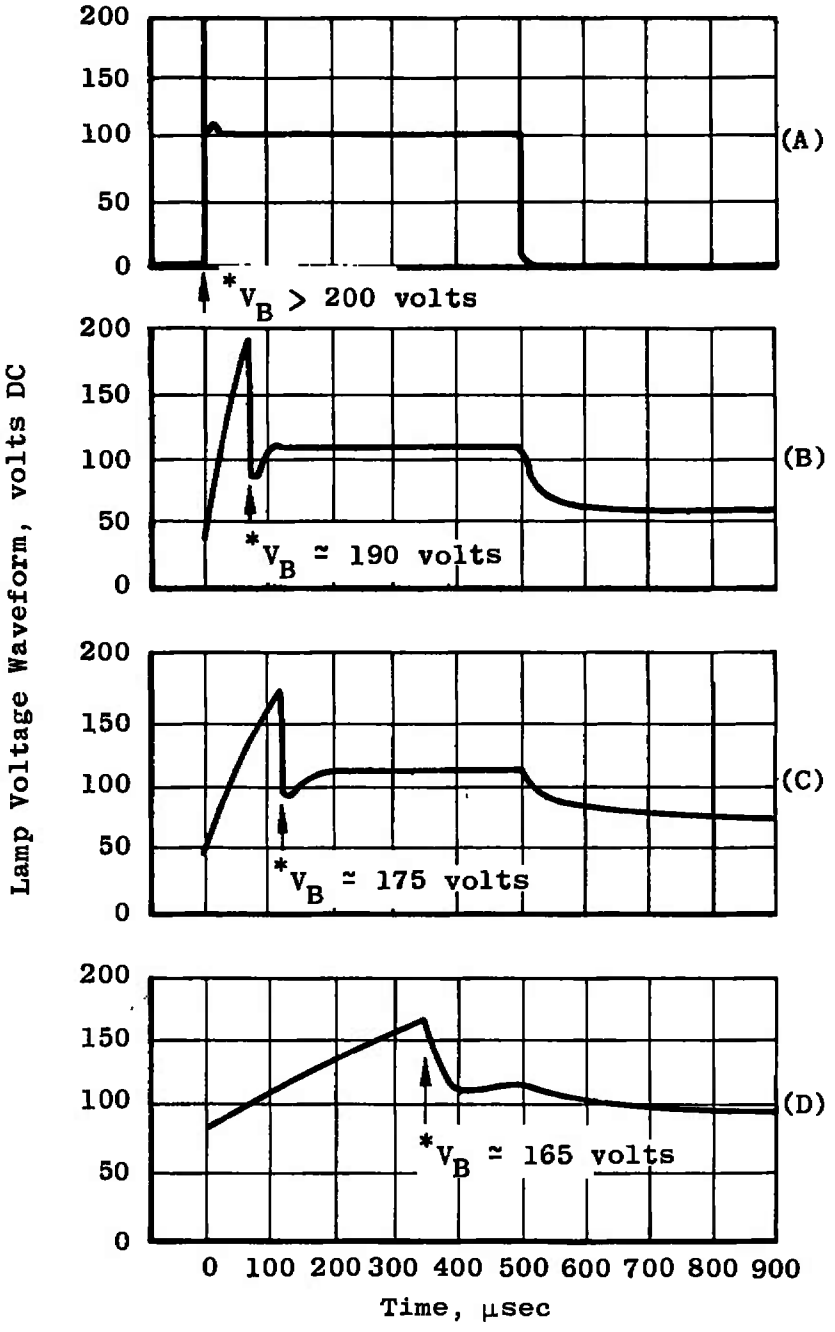

*Lamp Ionization Point

(A) Lamp Driven by a Short Cable, Low ΔCR_b Time Constant

(B)-(D) Progressive Increases in the ΔCR_b Time Constant

Fig. 8 General Form of Lamp Voltages Commonly Found in Timing Light Circuits Using Neon Lamps

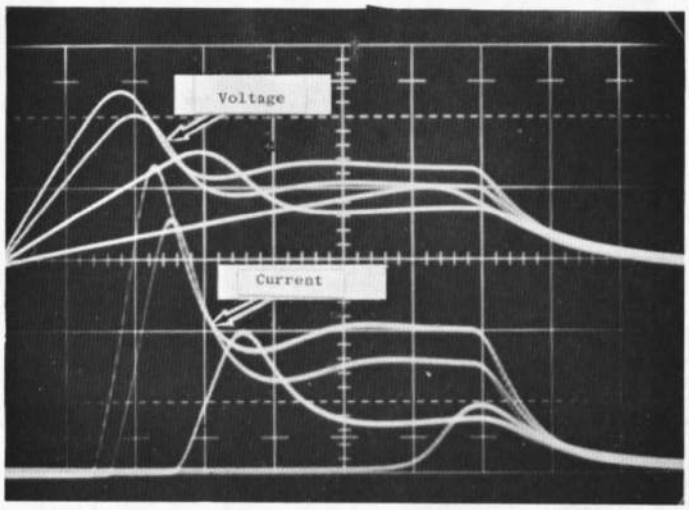

Horizontal Scale, 20 μsec/cm

Vertical Scale:

Top Trace; Lamp Voltage, 20 volts/cm

Lower Trace; Lamp Current, 10 ma/cm

NE51H at 1-KHz PRR Driven through 400-ft RG58 Cable via Ballast Resistors 13, 17, 33, and 100 KΩ with Corresponding Lamp Currents of 23, 17, 8, and 2.5 ma, Respectively; Zero Reference, Lower Line

Fig. 9 Lamp Voltage-Current Characteristics for Four $R_b \Delta C$ Time Constants

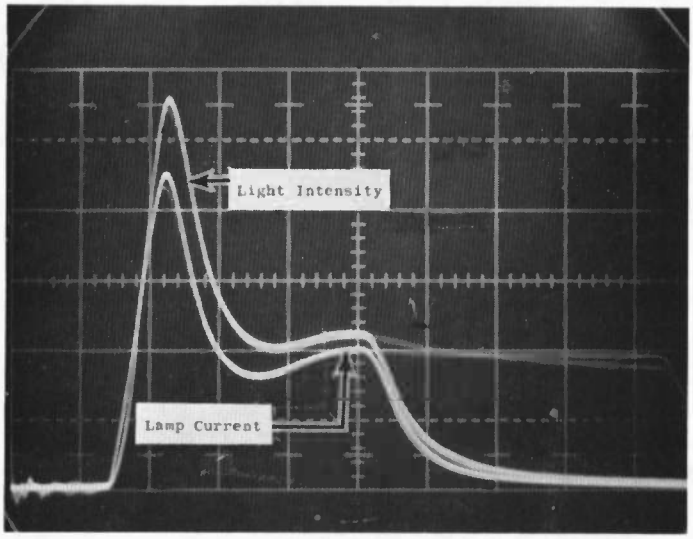

Horizontal Scale, 20 μsec/cm

Vertical Scale:

Top Trace; Lamp Intensity, Uncalibrated

Lower Trace; Lamp Current, 10 ma/cm

Fig. 10 Lamp Current versus Lamp Intensity

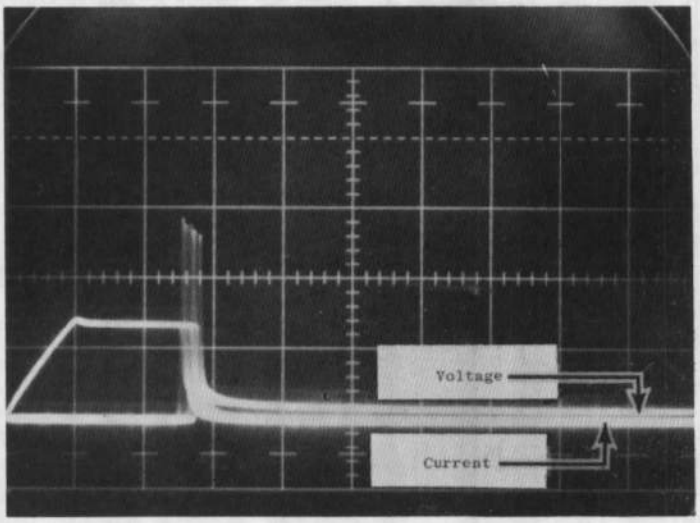

Horizontal Scale, 200 μsec/cm

Vertical Scale:

Voltage Top Trace, 50 volts/cm

Current Lower Trace, 20 ma/cm

Zero Reference, Current

Zero Reference, Voltage

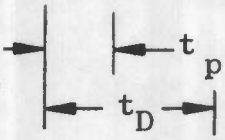

Lamp Ionizes 300 μsec after Termination of V_s, t_p = 200 μsec

Fig. 11 Undesirable Delayed Ionization Mode of the Neon Lamp

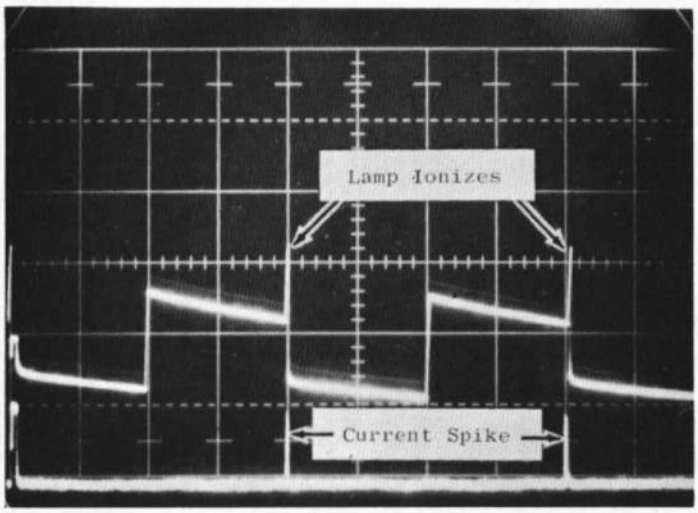

Horizontal Scale, 5 msec/cm

Vertical Scale:

Top Trace; Lamp Voltage, 50 volts/cm

Lower Trace; Lamp Current, 5 ma/cm

$V_s(t)$ with V_s = 375 volts

100-Hz Pulse Repetition Rate

V_s PRR, 100 Hz

Lamp PRR, 50 Hz

Fig. 12 Extreme Lamp Ionization Delay

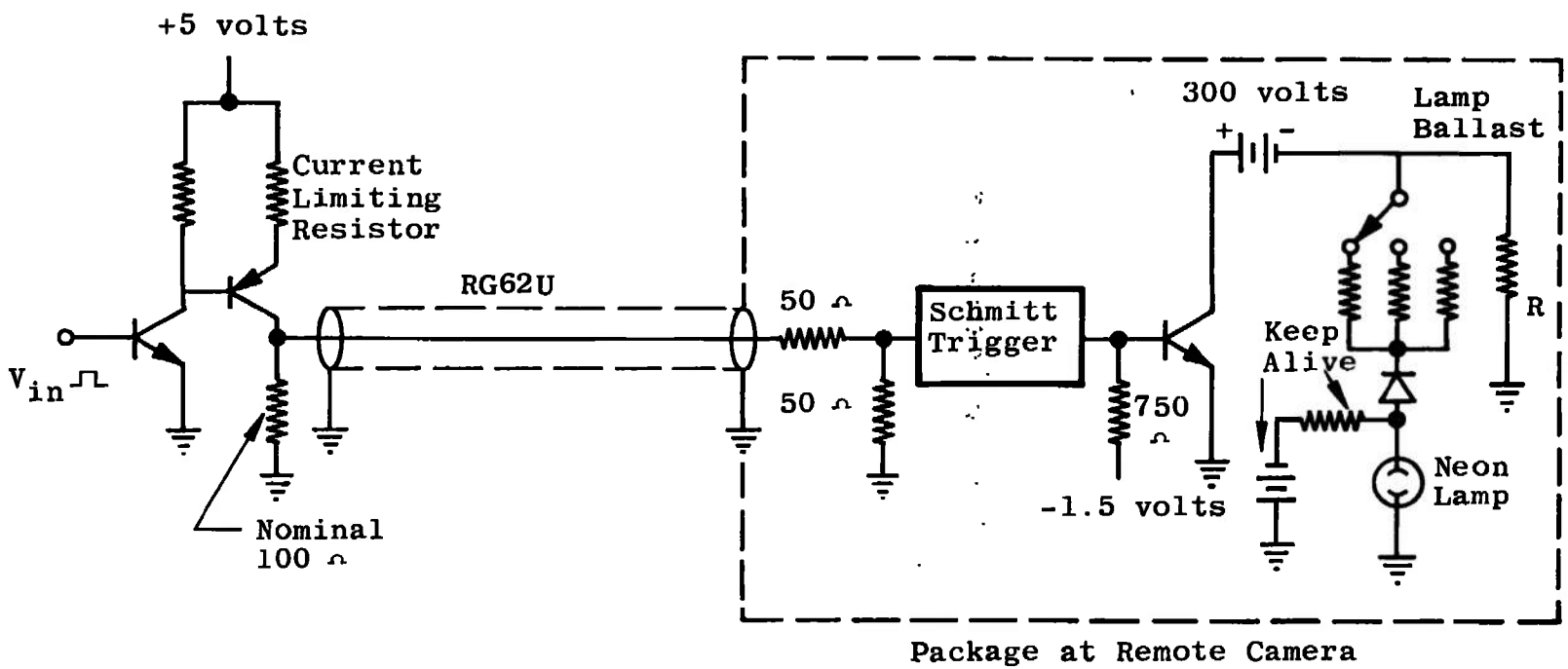

Fig. 13 Switching Transistor at the Camera

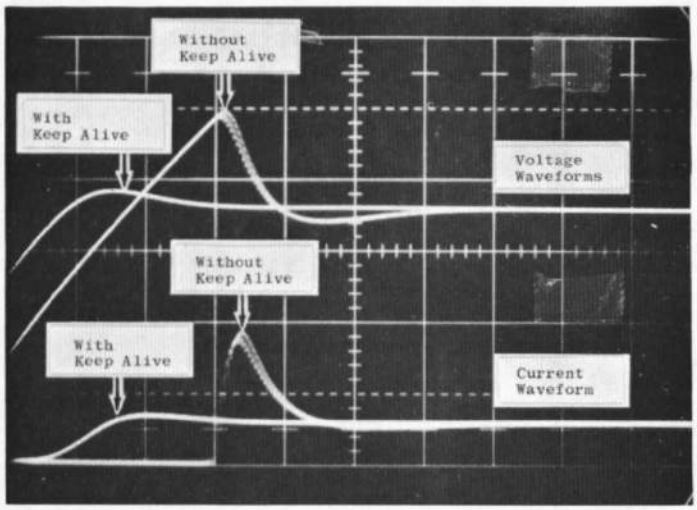

Horizontal Scale,
20 μsec/cm

Vertical Scale:

Top Trace; Lamp Voltage, 20 volts/cm

Lower Trace; Lamp Current, 10 ma/cm

NE51 Lamp Driven at 100-Hz PRR

Fig. 14 Effect of Keep Alive in Reduction of Lamp Ionization Delay

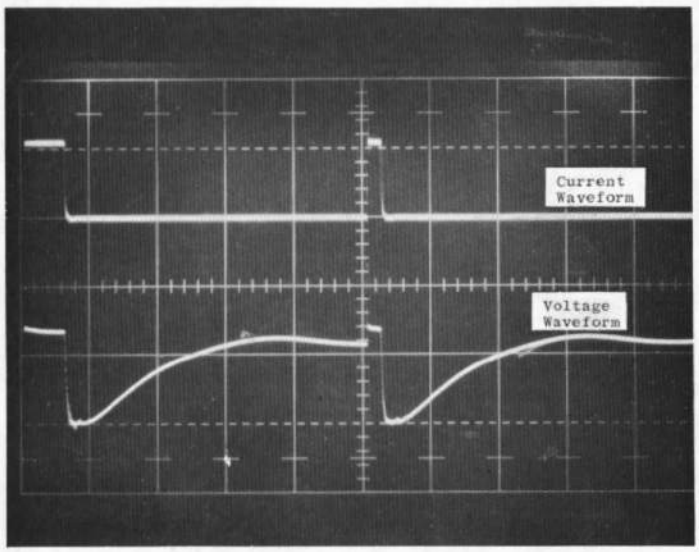

Horizontal Scale,
200 μsec/cm

Vertical Scale:

Top Trace; Lamp Current, 20 ma/cm

Lower Trace; Lamp Voltage, 50 volts/cm

Voltage Zero Reference, Lower Graticule Line

Ne51 Lamp Driven at 1000-Hz PRR
with 100-μa Keep-Alive Current

First pulse is a marker pulse.

Fig. 15 Lamp volt-amp Waveform, Lamp Driven with Keep Alive

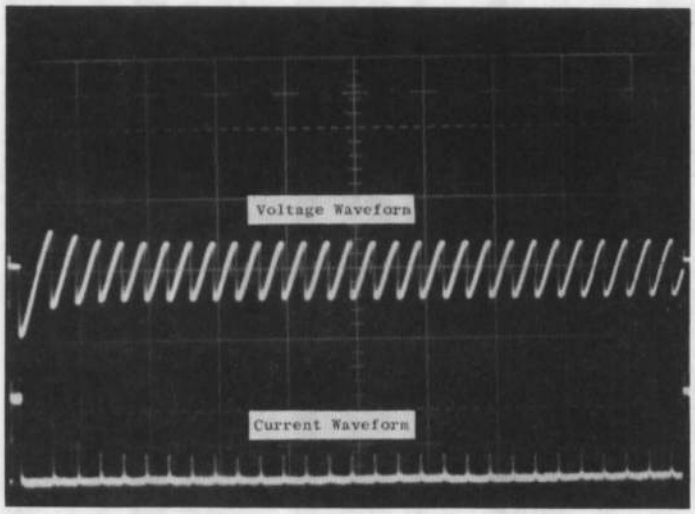

Horizontal Scale, 10 msec/cm

Vertical Scale:

Top Trace; Lamp Voltage, 20 volts/cm

Lower Trace; Lamp Current, 5 ma/cm

NE51H Lamp Driven at 10-Hz PRR

Fig. 16 Neon Lamp Relaxation Oscillation Problem

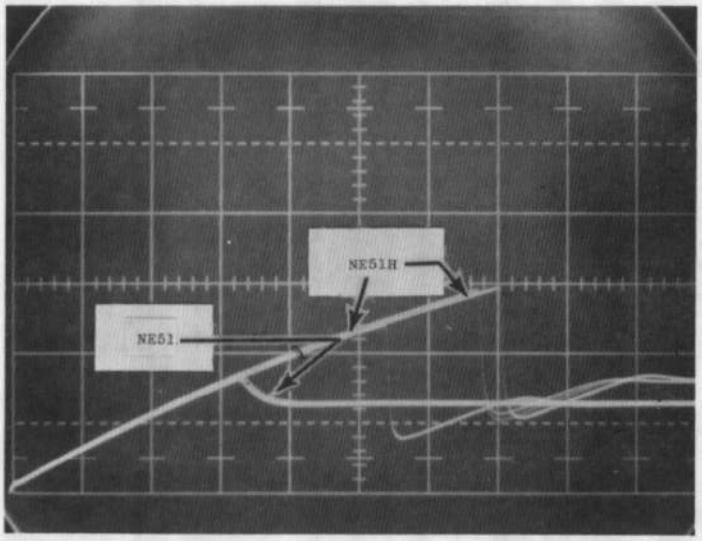

Horizontal Scale, 100 μsec/cm

Vertical Scale; Lamp Voltage, 50 volts/cm

Lamps Driven at 10-Hz PRR, $V_{ic} = 0$

Fig. 17 Comparison of the Dynamic Breakdown Voltages for NE51 and NE51H Lamps with Large $R_b \Delta C$ Time Constants

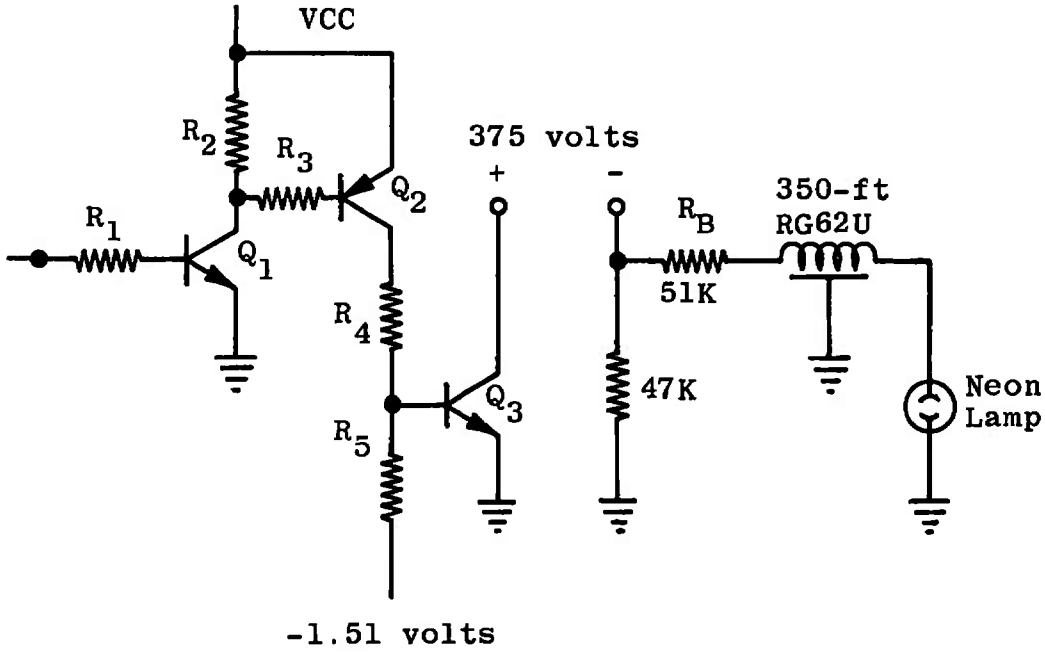

a. Conventional Circuit

Fig. 18 Comparison of Conventional Circuit to Dynamic Ballast

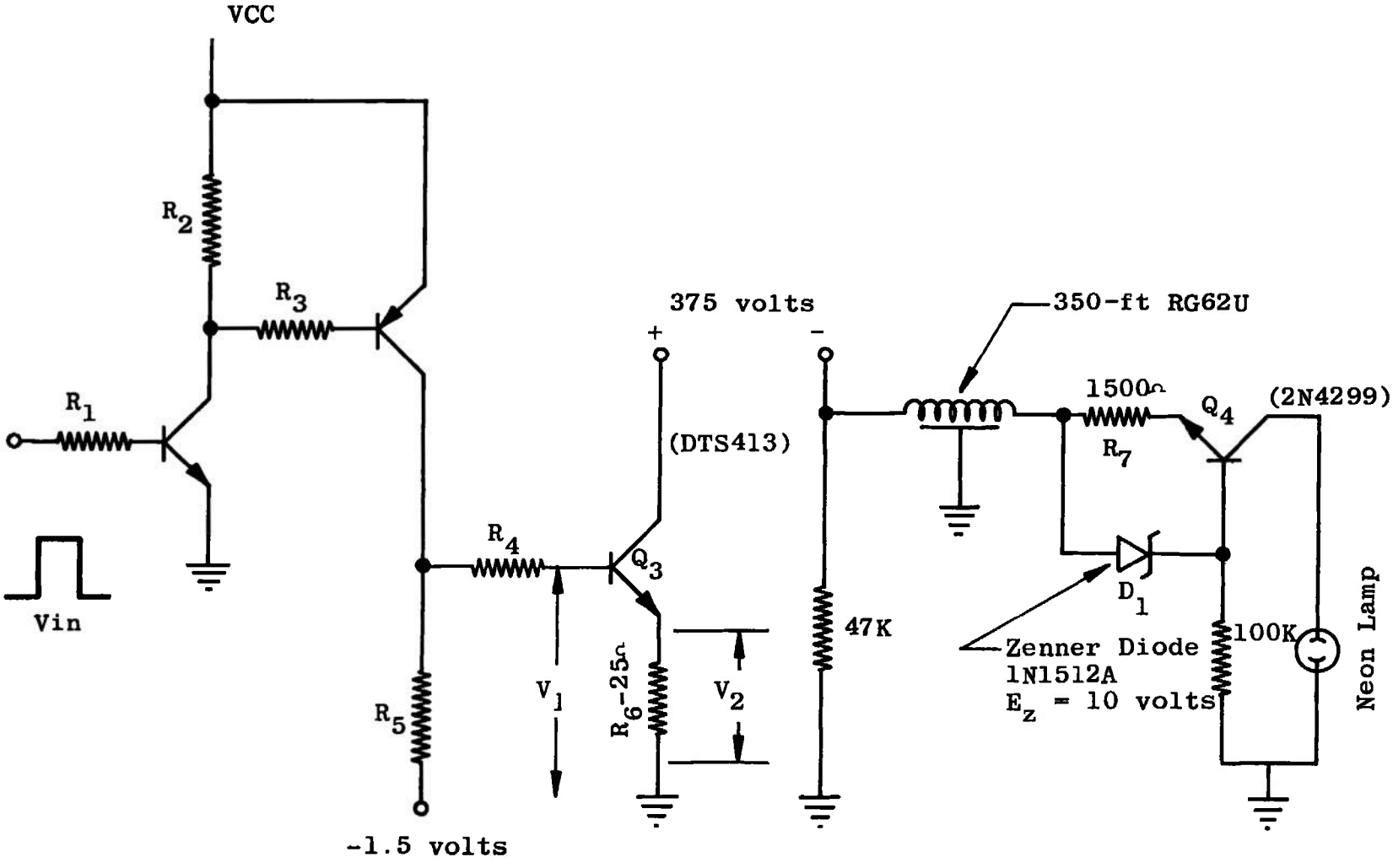

b. Dynamic Ballast and Current Limiting Circuit
Fig. 18 Continued

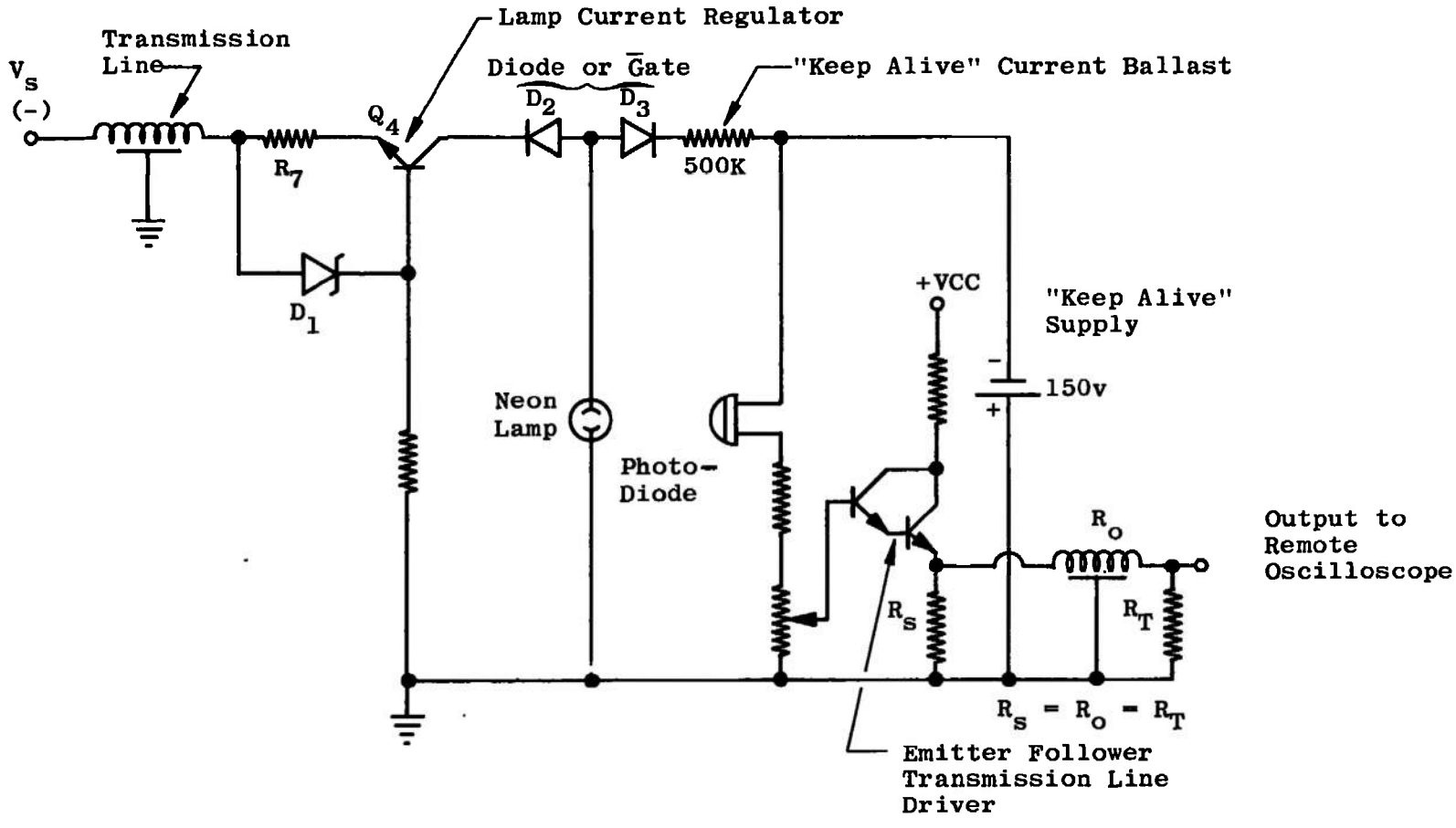

c. Keep Alive and Photodiode Monitor Addition to Fig. 18b

Fig. 18 Continued

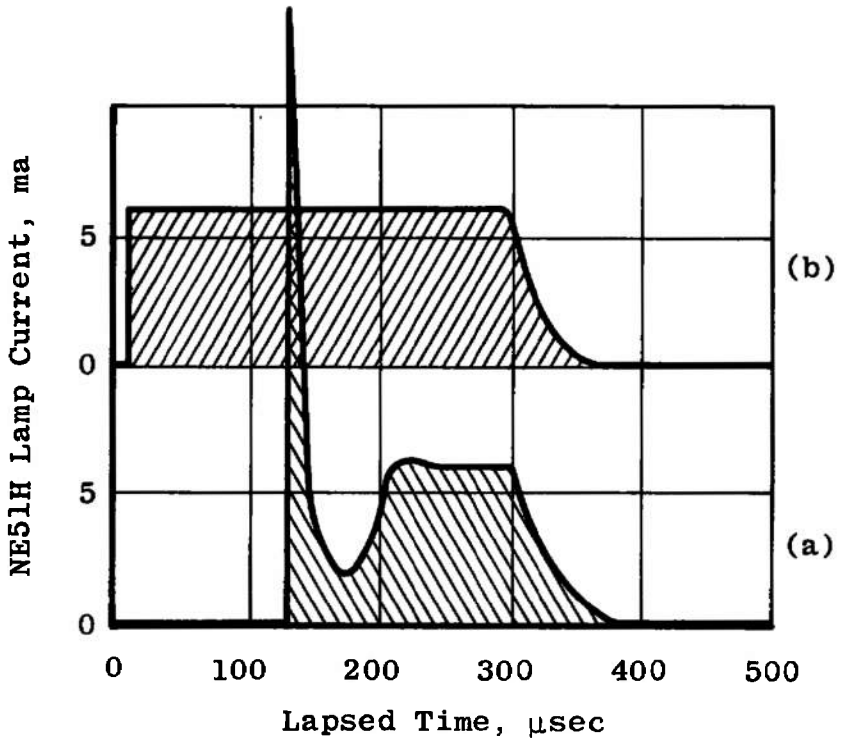

d. Lamp Current Pulse Produced by the Two Circuits; Pulse (a) Produced by Circuits 18a, Pulse (b) by Circuit 18b

Fig. 18 Concluded

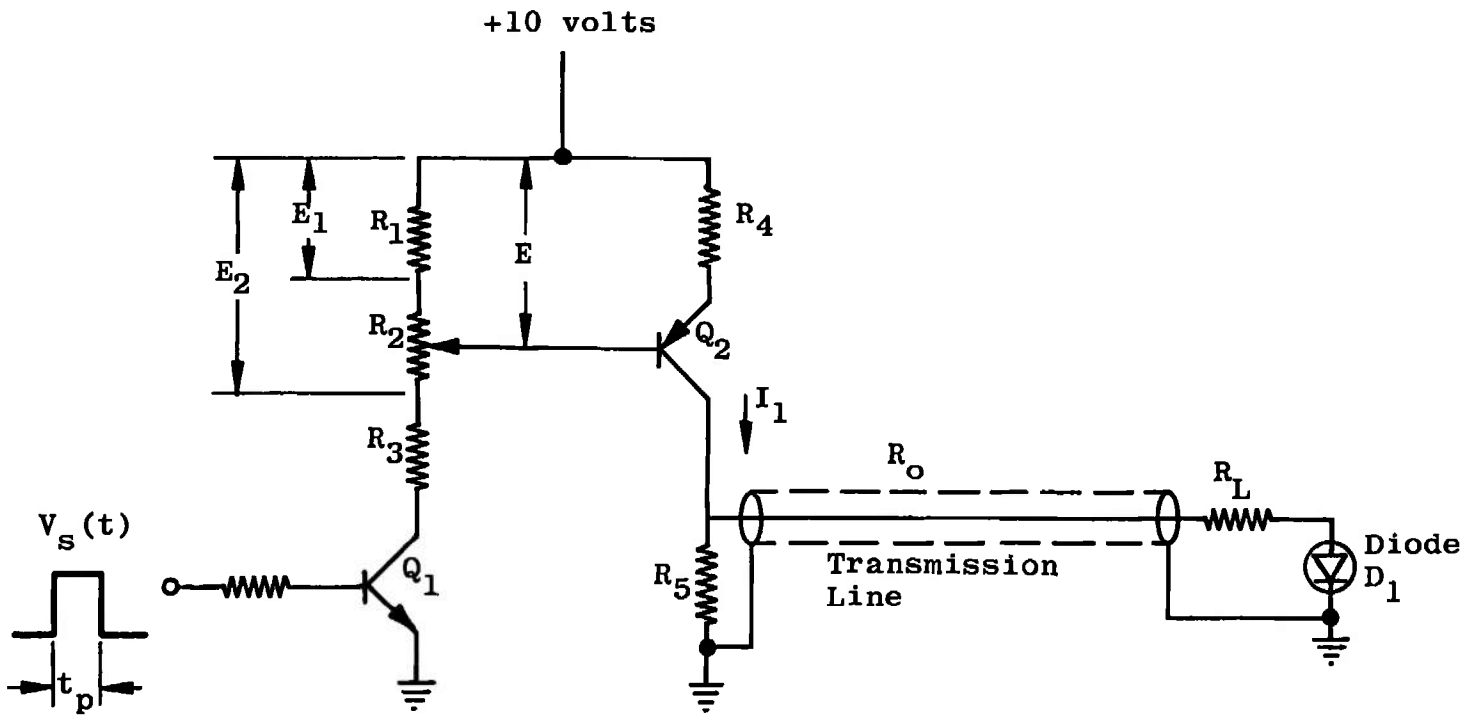

Fig. 19 Solid-State Light Emitting Diode Driver Circuit

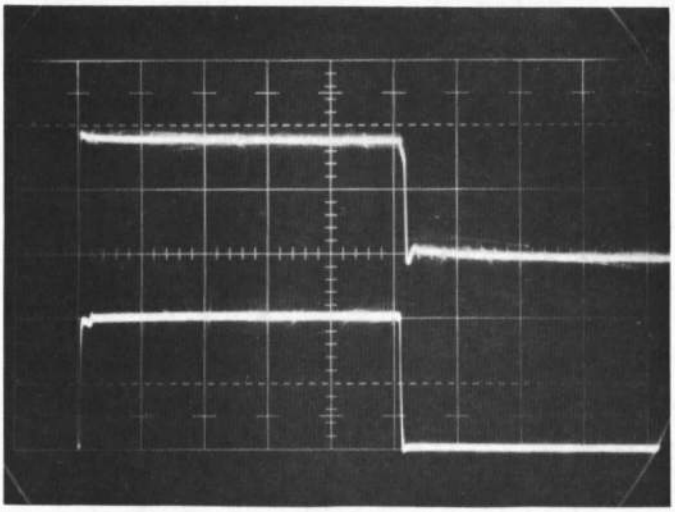

Horizontal Scale,
5 μsec/cm

Vertical Scale:

Top Trace; Voltage across the Diode, 1 volt/cm

Lower Trace; Diode Current, 50 ma/cm

a. LED Voltage and Current Waveforms; Driving Pulse Duration, 25 μsec at 1-KHz PRR

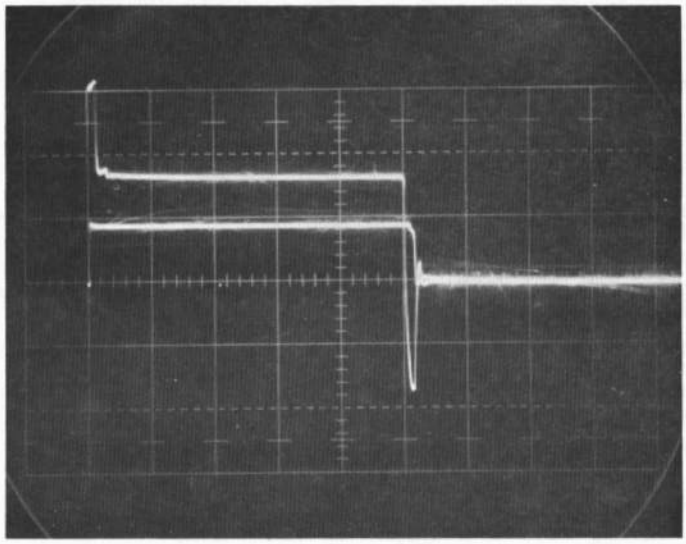

Horizontal Scale,
5 μsec/cm

Vertical Scale:

Top Trace; Voltage at Sending End of 300-ft Transmission Line, 2 volts/cm

Lower Trace; Voltage across the Diode at Receiving End of the Line, 2 volts/cm

1-KHz PRR

b. Sending End and Terminal End Voltage Waveforms; Driving Pulse Duration, 25 μsec at 1-KHz PRR

Fig. 20 Waveforms for a Gallium Arsenide Phosphide Light Emitting Diode Driven at the Terminal End of a 300-ft RG62 Transmission Line

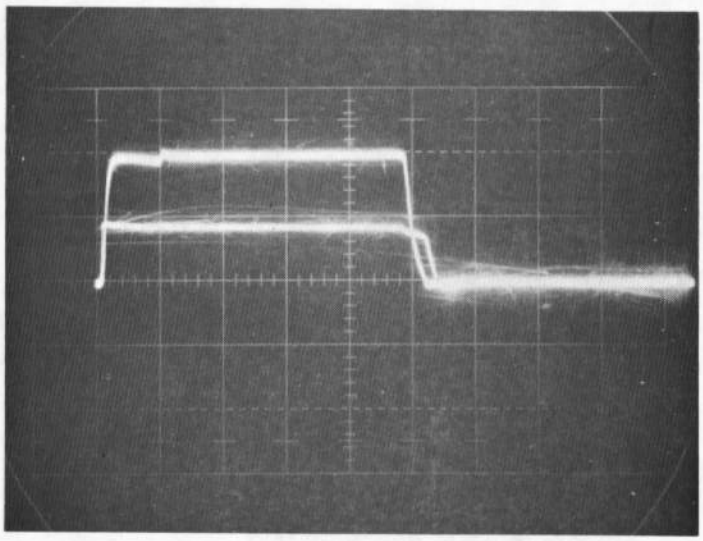

Horizontal Scale,
1 μsec/cm

Vertical Scale:
Top Trace; Diode Current, 50 ma/cm

Lower Trace; Voltage across Diode, 2 volts/cm

c. LED Driven at 10-KHz PRR by a 5-μsec Driving Pulse at the Terminal End of a 300-ft Transmission Line

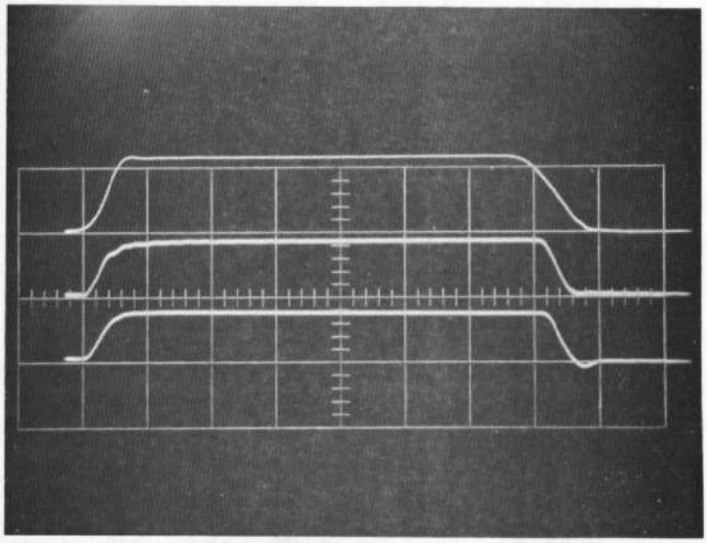

Horizontal Scale,
0.1 μsec/cm

Vertical Scale:

Top to Bottom;
1 volt/cm,
1300 ft lamberts/cm,
200 ma/cm

1. Voltage Pulse Output of Pulse Generator, Shows Rise Time Limitation of Generator < 50 nsec

2. Light Output of LED Approximately 1000 ft lamberts

3. LED Current during Pulse Generator Voltage Pulse

d. LED Driven at 200-KHz PRR by a 0.7-μsec Duration Pulse

Fig. 20 Concluded

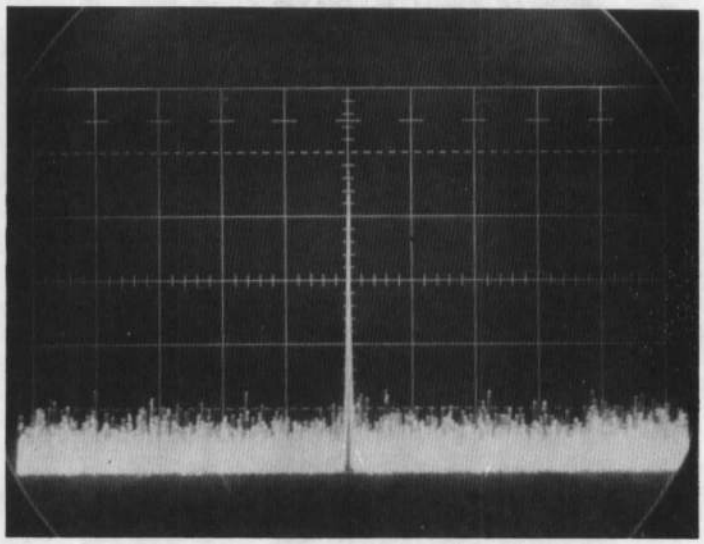

95 94 93 92 91 90 89 88 87 86 85

MHz

Spectrum Analyzer Conditions

1. Center Frequency, 90 MHz
2. Dispersion, 1 MHz/cm
3. Displayed 90-MHz Signal Power, -70 dbm

Fig. 21 Gallium Arsenide Phosphide Diode Driven at 90-MHz Rate

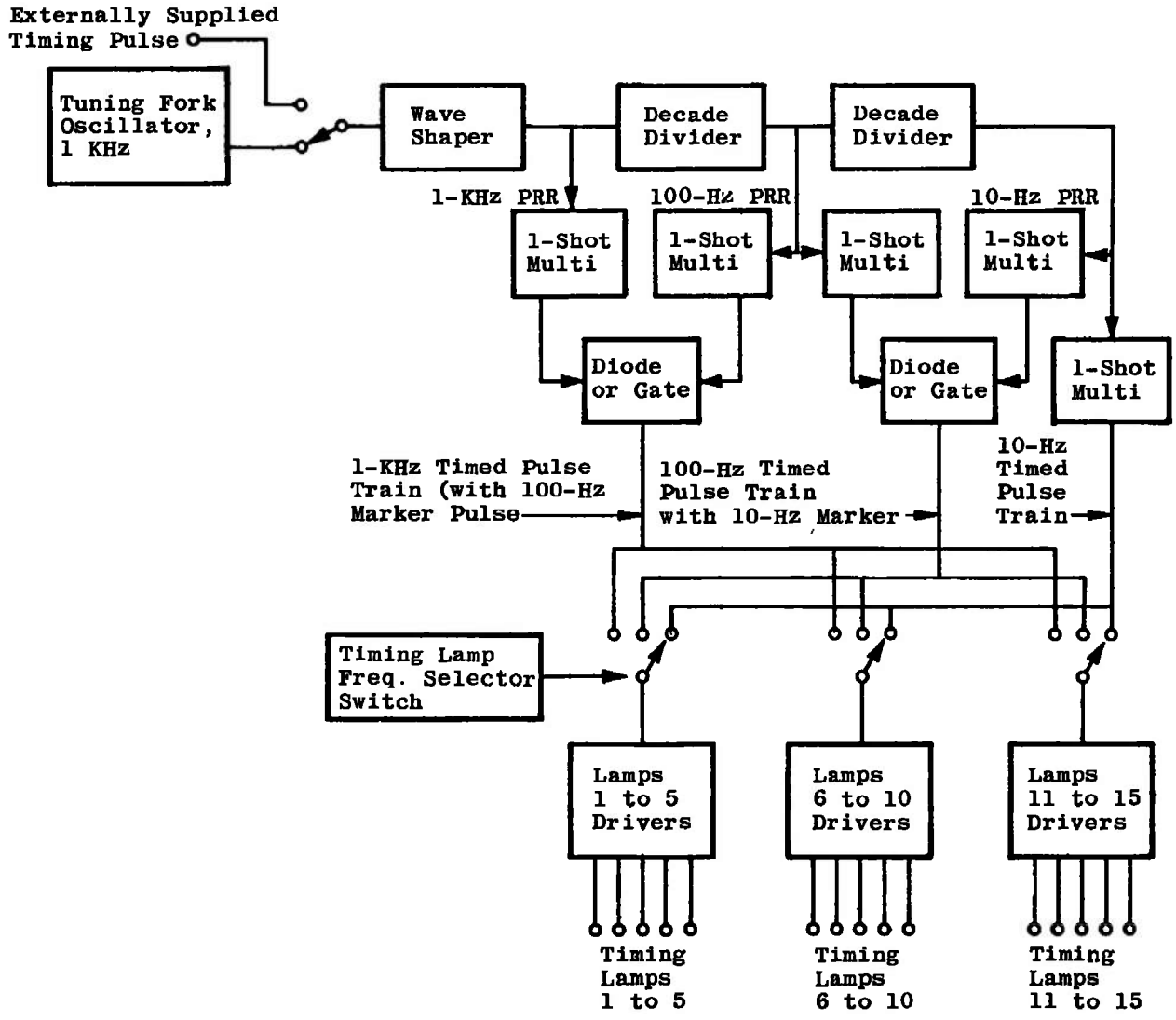

Fig. 22 Block Diagram of a 15 Camera Timing Light Generator

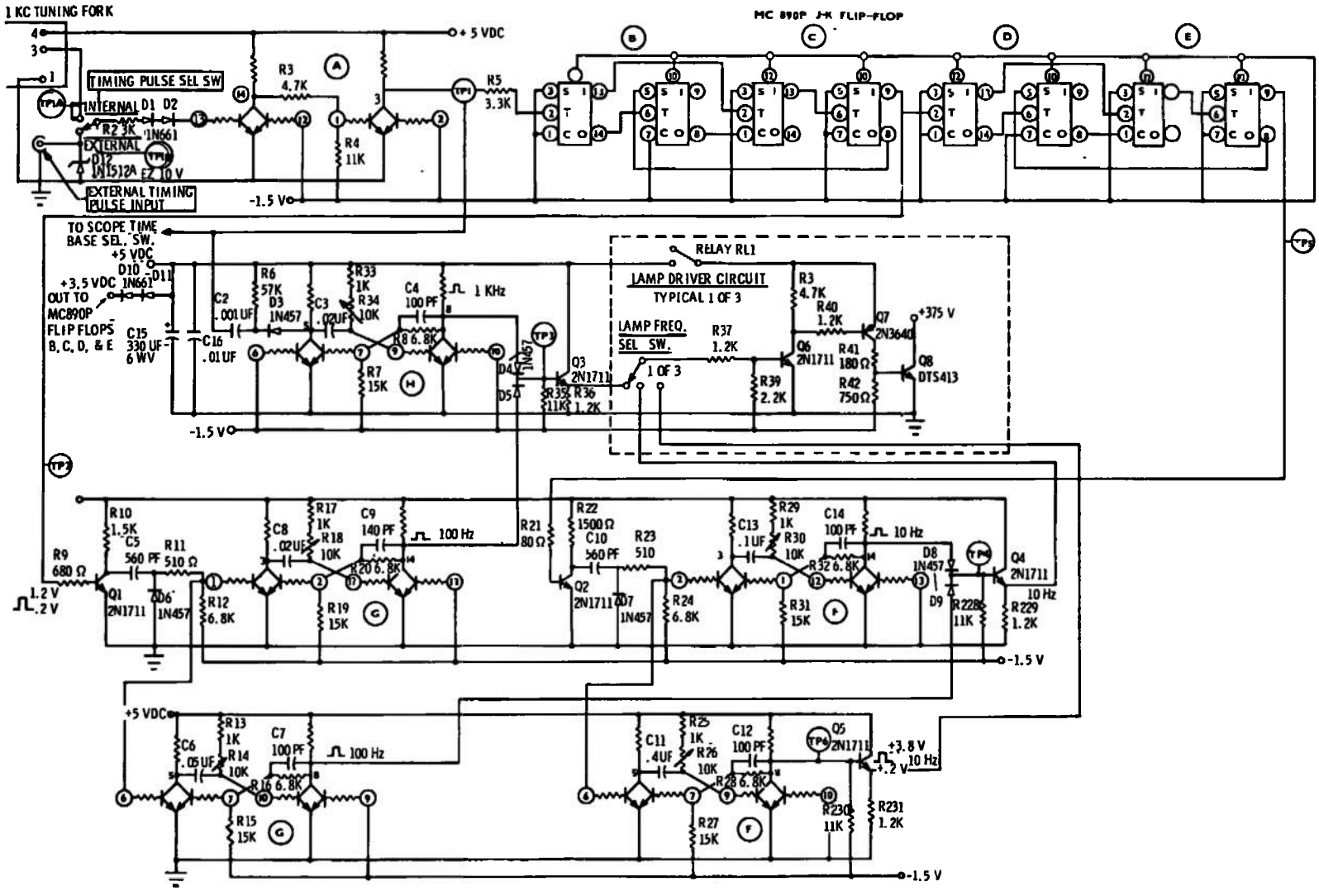

Fig. 23 Timing Logic Circuit

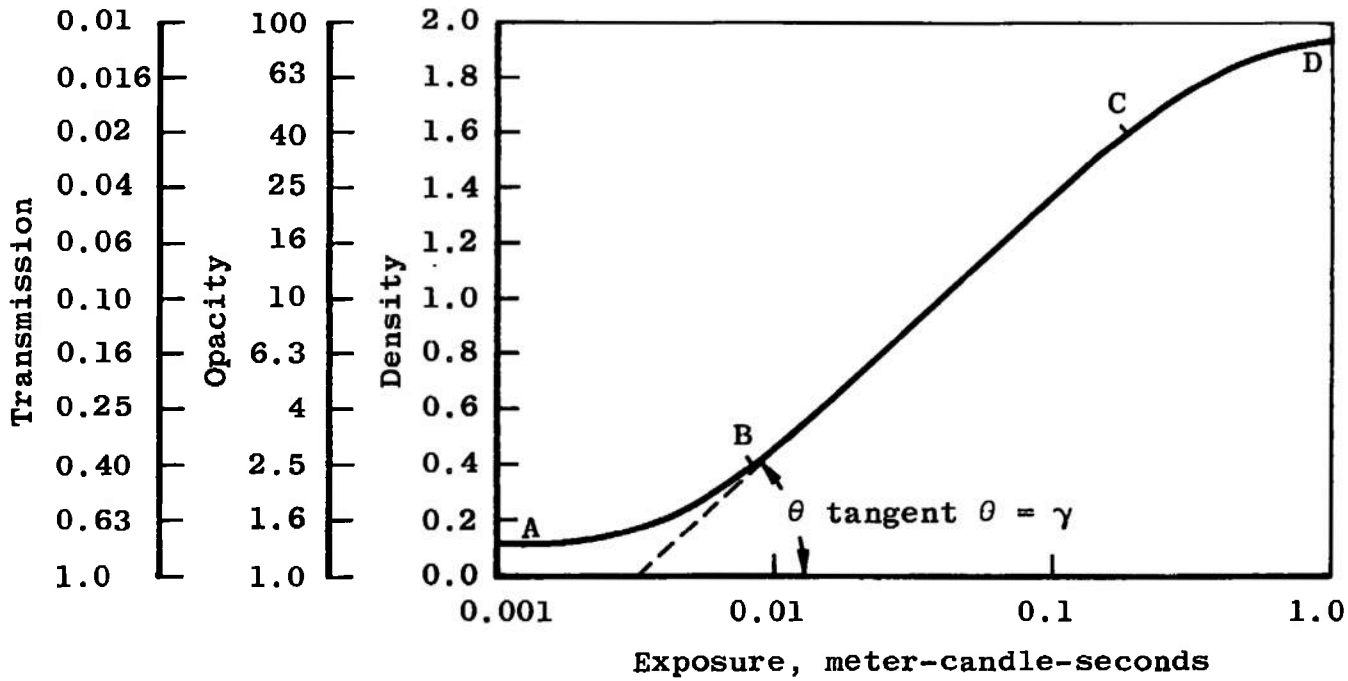

A-B: Toe, Minimal Exposure

C-D: Shoulder, Maximum Exposure

Fig. 24 General Characteristics Curve for Photographic Film

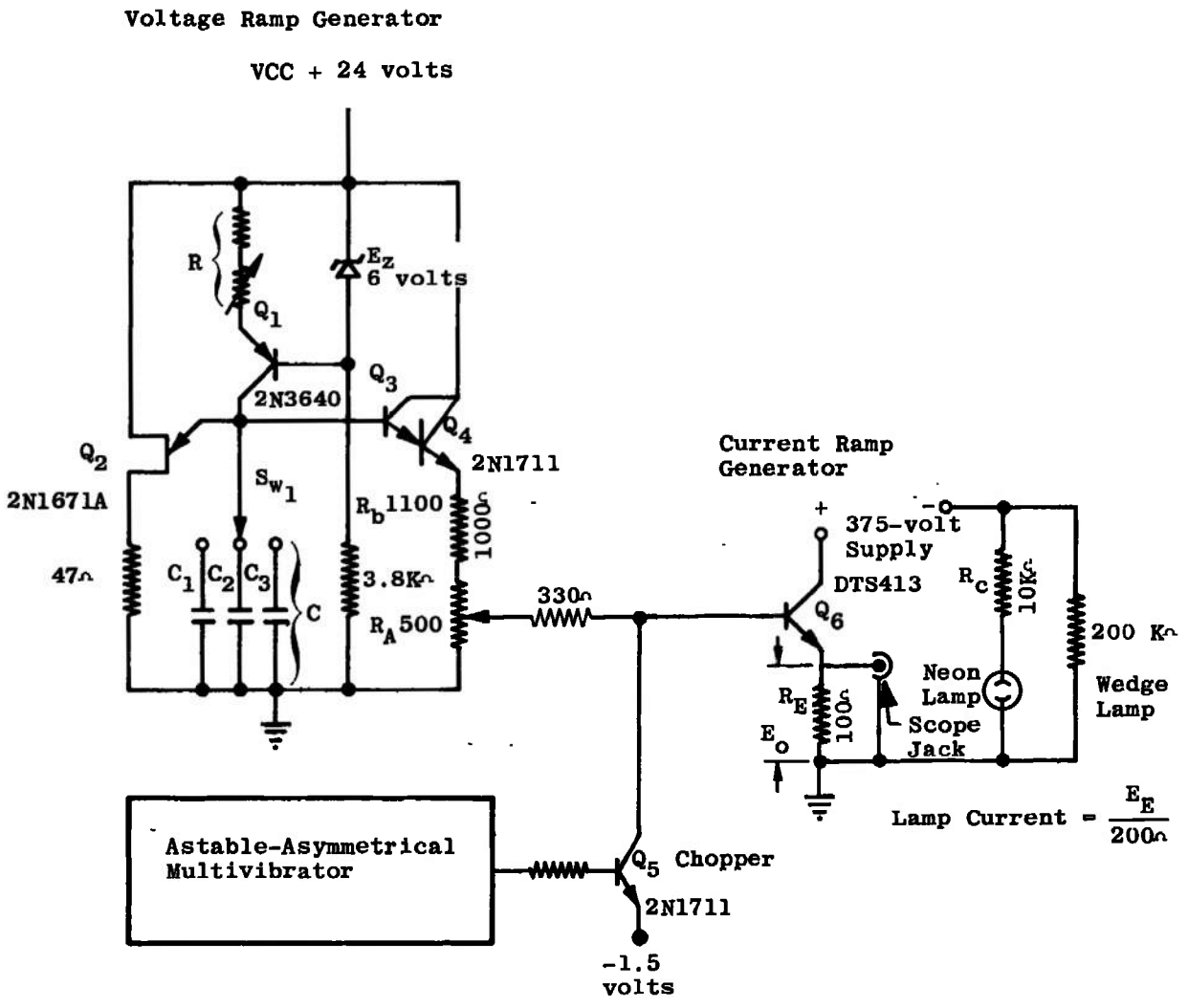

Fig. 25 Current Ramp-Density Wedge Generator

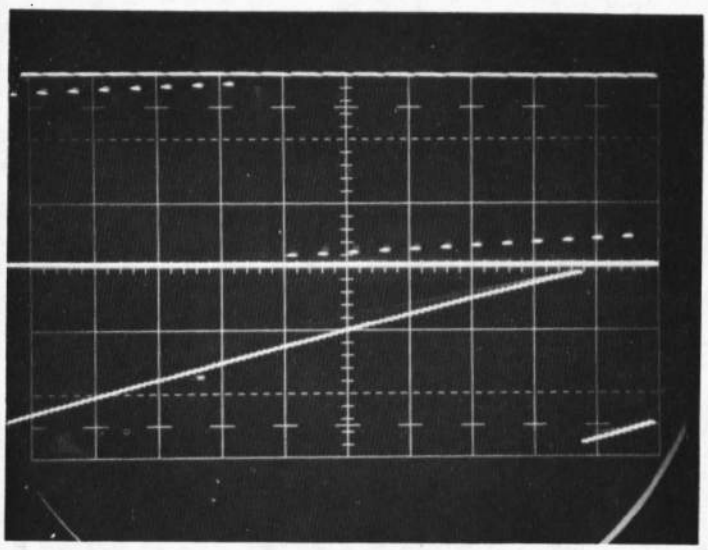

Vertical Scale,
10 ma/cm

Horizontal Scale:

Top Trace;
10 msec/cm

Lower Trace;
2 msec/cm
(Illustrates Ramp Transition on Expanded Time Scale)

Fig. 26 Series of Lamp Current Pulses of Linearly Increasing Amplitude

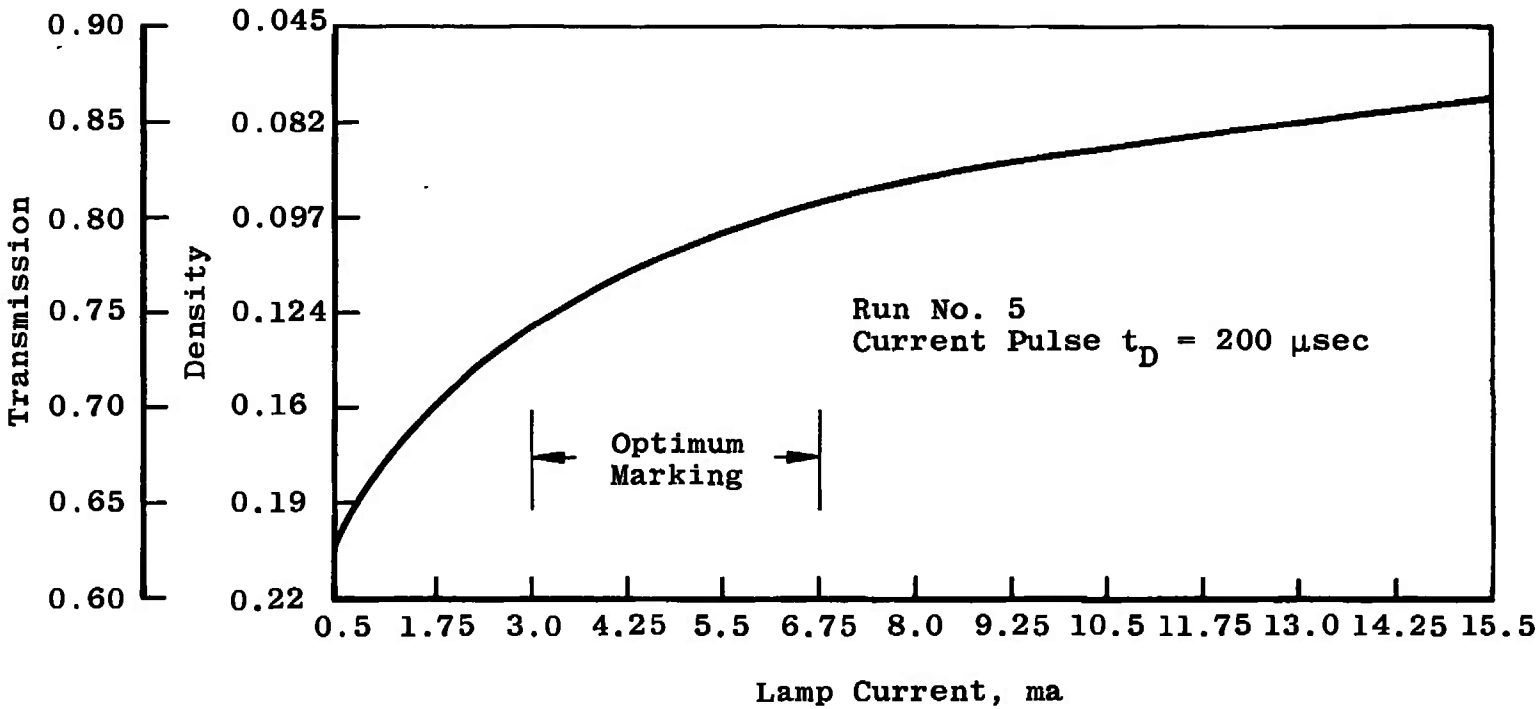

Fig. 27 Density versus Lamp Current for 7258 Color Reversal Film

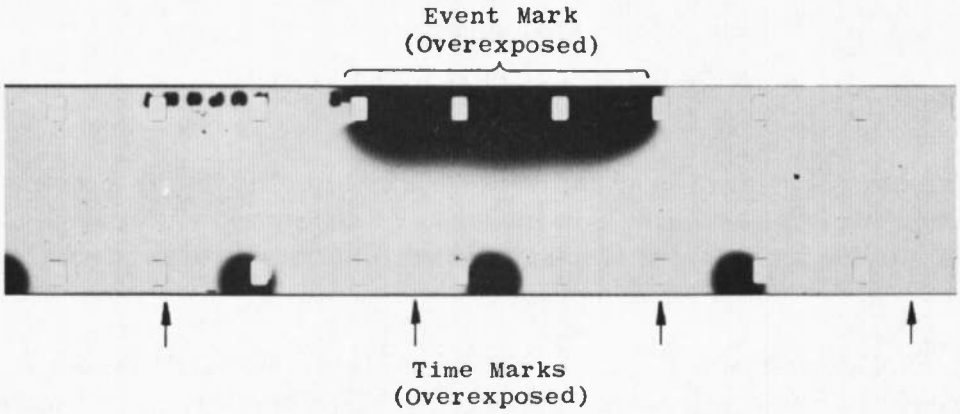

a. No Light Collimating Devices Used

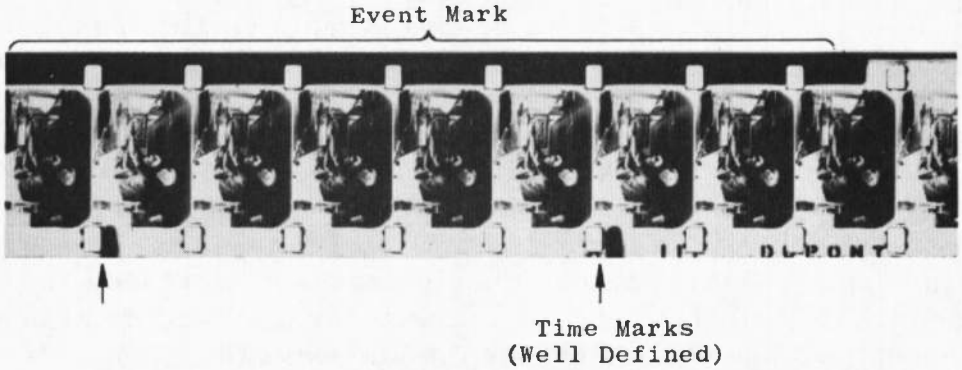

b. Light Collimating Lens and Precision Slit Used

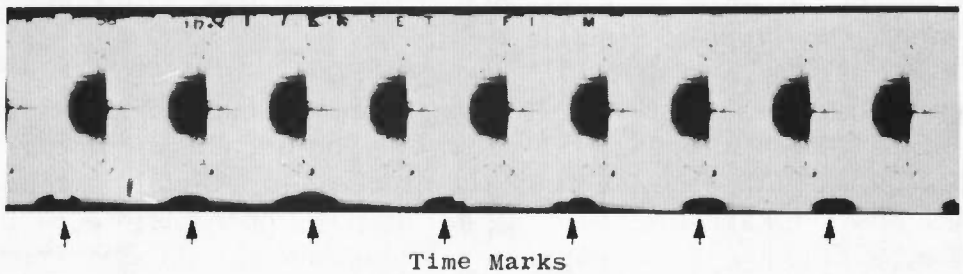

c. No Light Collimating Devices Used

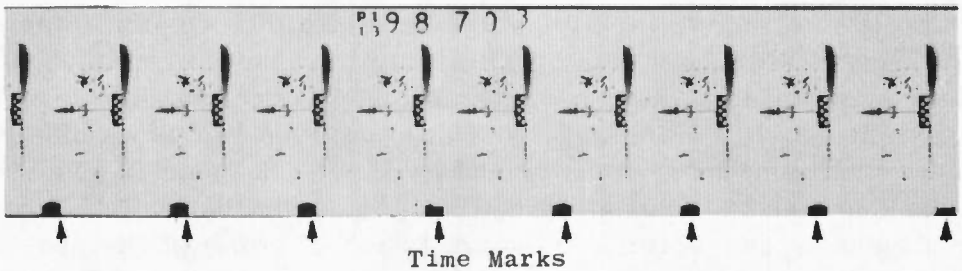

d. Light Collimating Device Used

Fig. 28 Samples of Timing Marks Produced with and without Light Collimating Devices

APPENDIX II
NEON GLOW LAMP CHARACTERISTICS

The neon glow lamp is classified as a cold cathode gas discharge device consisting of two alkali oxide or barium compound coated electrodes sealed in a glass envelope filled with neon gas to moderately low pressure.

The application of a potential between electrodes will cause a migration of residual ions to produce a current. The magnitude of this current depends on the rate of production of ions by external ionizing agents and the migration of positive ions to the cathode and is governed by the electric field. This current in the NE51H is quite small, less than 1 μA, and is termed the "dark current" since very little glow is apparent. The magnitude of the dark current, however, can vary appreciably between a lamp in total darkness and one exposed to external light because of the photomissive effect or emission of electrons caused by incident radiation on the electrode coating.

As the applied voltage across the electrodes is increased, a point is reached (B, Fig. II-1) where the current (threshold current) begins to rise abruptly. The voltage across the lamp will then drop to a lower value (C, Fig. II-1) governed by the value of the external "ballast" resistance. This rapid increase in current above the dark current level is the result of ionization of gas molecules by collision with electrons accelerated by the applied electric field.

The voltage present across the lamp when the current starts to rise is defined as the static breakdown voltage. The breakdown voltage is influenced by the following factors: the electrode material, composition of the gas, age and method of aging lamp (cathode disintegration by ion bombardment), electrode temperature, and the interdependency between interelectrode spacing and gas pressure.

No single current-voltage curve would suffice to describe the behavior of a particular glow lamp. The lamp may be said to have static characteristics and dynamic characteristics. Static breakdown voltage values assigned by the manufacturer to the various lamps as used for film time marking are 90V for the NE51 (B1A), 135V for the NE51H (B2A), 135V for NE2J (C9a) and NE2H (C2A), and 90V for NE66. Breakdown of the gas is characterized by excitation of some of the gas atoms, which subsequently emit radiation as they return to a state of lower energy. The "glow discharge" applies to this visible radiation. Following breakdown, the characteristic curve passes through a transition

region called the negative resistance region. Operation of a lamp such that it (repeatedly) passes through this region is typical of a relaxation oscillator.

The lamp is a bistable device, in that it is stable on either side of the negative resistance area. Presence of the lamp in an extremely high illumination level may eliminate this negative resistance characteristic.

With further increase in current, the lamp enters the normal glow region where the glow covers only a portion of the cathode and the current is confined to the portion of the cathode that glows. The minimum maintaining voltage of the lamp is found here. The lamp resembles a constant voltage device in this region.

As the current through the lamp increases further, the cathode surface becomes covered by glow, and the cathode drop and the current density increases. This is termed the abnormal glow region. The neon timing light is operated far into this region for short periods of time. Sustained operation in the upper limits of this region (E-G, Fig. II-1) will result in overheating the cathode, with a transition of the glow into an arc (F, Fig. II-1).

The glow lamp must have a series current limiting resistance in the circuit to protect the lamp. The particular value of ballast resistance used in combination with the applied voltage and lamp characteristics determines the current through the lamp and, in turn, its life and light output. Neon lamps are made as standard brightness (primarily stable electrical characteristics, example NE51) and high brightness types (primarily maximum light output, example NE51H). The light output of all glow lamps varies in direct proportion to the current through the lamp. The light from the NE51, NE51H, NE2J, and NE2 is confined mainly to the yellow and red regions of the spectrum between 5700 and 7500 angstroms.

The standard brightness lamp additionally emits some light at 5200 to 5400 Å. The efficiency of the standard brightness type is low, averaging about 0.06 lumens/ma. The high brightness type averages 0.15 lumens/ma, about three times that of the standard brightness. Because of the ability of the high brightness lamp to withstand higher currents, its light output is about ten times that of the standard brightness lamp, when the two are compared on an equal life basis (Ref. 4).

The useful life of the standard brightness lamp is limited by slow bulb blackening with reduction in light output and a gradual rise in breakdown and maintaining voltages. The blackening of the bulb is the

result of sputtering or disintegration of the cathode surfaces from ion bombardment and the deposition of these particles on the glass surface. The increase in breakdown voltage is also caused by the destruction of the cathode coating, with resultant reduction in free charge carriers. The high brightness lamp aging characteristics are somewhat different than the standard brightness lamp. Instead of a gentle rise in breakdown voltage throughout life, the high brightness lamp near end of life experiences an abrupt upward change in breakdown and maintaining voltage.

The NE51 is rated nominally at 1/25 watt and 0.3 ma where the NE51H is rated nominally at from 1/7 to 1/4 watt and from 1.2 to 1.9 ma; the NE2J is rated at from 1/4 watt and 1/8 ma.

As stated earlier, the cathode surface material is photosensitive, and its emission can be greatly reduced by the absence of illumination. Glow lamps in total darkness become erratic and may require many volts in excess of usual static values to start them. Mild radioactive additives are used in many lamps to greatly reduce this effect.

The ionization time is defined as the time required for full-operating current and light output to be obtained following the application of a step voltage pulse to a nonconducting lamp.

The ionization time (Ti) is the sum of the statistical time (ts) required for the first free electron to form in the gas and the avalanche time (ta) needed for the first free electron to create the full flow of electrons. These time intervals are shown in Fig. II-2.

The statistical time is a function of the general state of excitation of the electrons at the time the pulse is received. This, in turn, is a function of the excitation remembered from recent on states and environmental factors such as the ambient light level, electric field strength, and the impressed potential on the electrodes. It is also a function of various construction properties such as gas composition and isotope content. Avalanche time (t_a) depends mainly on just the circuit-imposed electrode potential (Ref. 11).

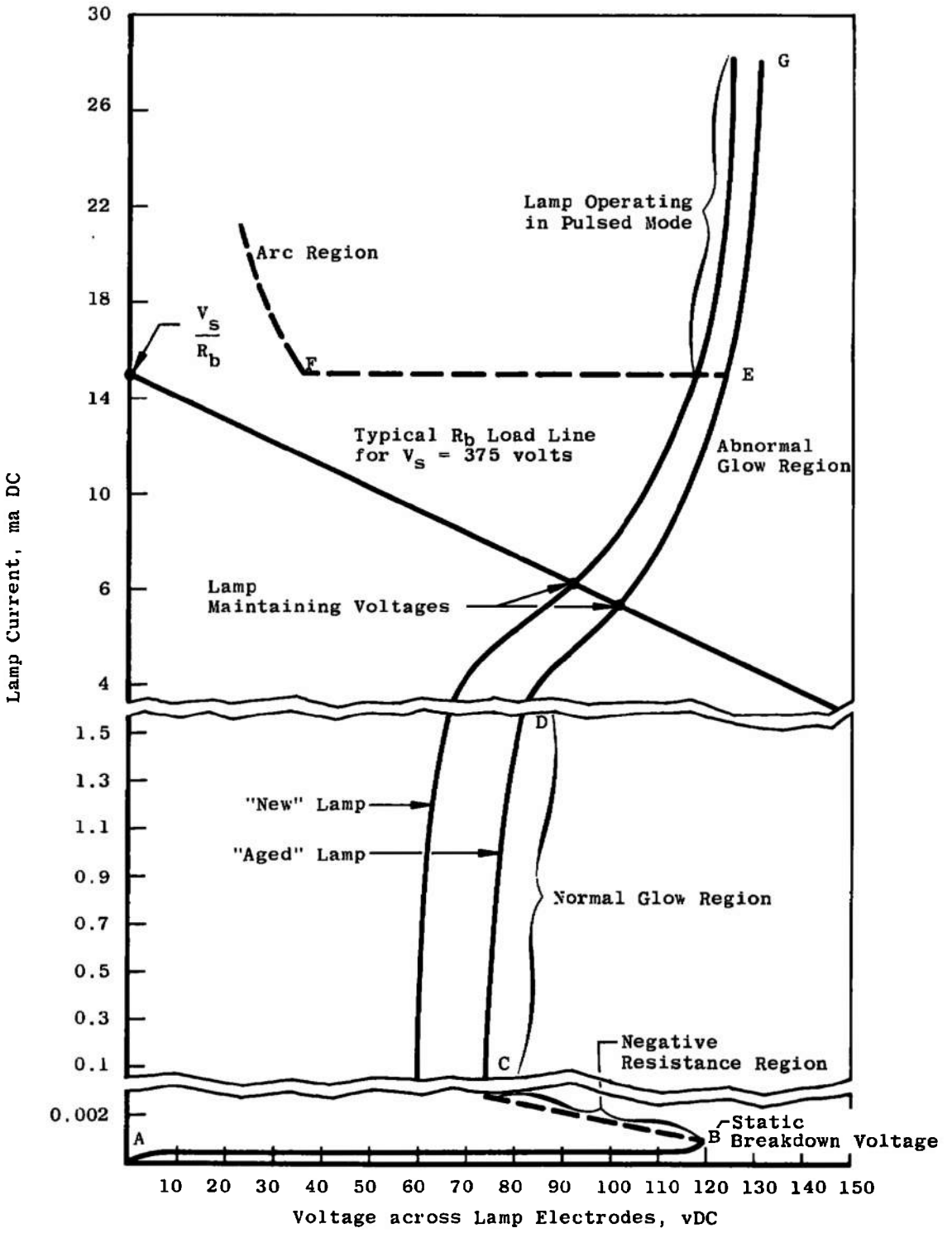

Fig. II-1 Static Characteristics of an NE51H Lamp

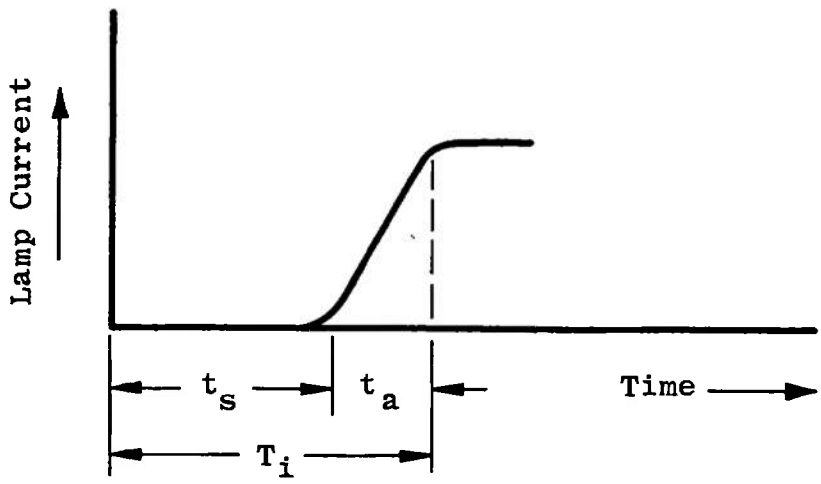

Fig. II-2 Neon Glow Lamp Ionization Characteristics

UNCLASSIFIED
Security Classification

DOCUMENT CONTROL DATA - R & D

(Security classification of title, body of abstract and indexing annotation must be entered when the overall report is classified)

1. ORIGINATING ACTIVITY *(Corporate author)*
Arnold Engineering Development Center
ARO, Inc., Operating Contractor
Arnold Air Force Station, Tennessee

2a. REPORT SECURITY CLASSIFICATION
UNCLASSIFIED

2b. GROUP
N/A

3. REPORT TITLE
TIME-MARKING HIGH-SPEED FILM IN MULTIPLE-CAMERA INSTALLATIONS

4. DESCRIPTIVE NOTES *(Type of report and inclusive dates)*
Final Report - January to May 1968

5. AUTHOR(S) *(First name, middle initial, last name)*
H. T. Kalb and F. L. Crosswy, ARO, Inc.

6. REPORT DATE
June 1970

7a. TOTAL NO. OF PAGES
78

7b. NO. OF REFS
11

8a. CONTRACT OR GRANT NO. F40600-69-C-0001

b. PROJECT NO.

c.

d.

9a. ORIGINATOR'S REPORT NUMBER(S)
AEDC-TR-70-168

9b. OTHER REPORT NO(S) *(Any other numbers that may be assigned this report)*
N/A

10. DISTRIBUTION STATEMENT
This document has been approved for public release and sale; its distribution is unlimited.

11. SUPPLEMENTARY NOTES
Available in DDC.

12. SPONSORING MILITARY ACTIVITY
Arnold Engineering Development Center, Air Force Systems Command, Arnold Air Force Station, Tenn.

13. ABSTRACT
The general time-event correlation problem for high-speed (10,000-frames/second), motion analysis cameras is discussed. The specific optics, sensitometry, and electronics problems involved in placing precise time and event marks on high-speed film, in addition to the design and development of an operational time and event signal generator, are discussed. The generator features a tuning fork time standard, integrated circuit timing logic that can furnish independent time and event signals for up to 15 cameras. A current ramp-film density wedge generator is presented as a novel method for relating time-mark lamp current amplitude to film-mark density. Recently developed, solid-state, light emitting diodes (LED) were investigated for application to the time-mark problem. The LED proved capable of providing time-marking pulses at rates in excess of 200 kHz. A technique for analyzing a waveform to operationally test the neon lamp timing circuit is evaluated.

DD FORM 1 NOV 65 1473

UNCLASSIFIED
Security Classification

14. KEY WORDS	LINK A ROLE	LINK A WT	LINK B ROLE	LINK B WT	LINK C ROLE	LINK C WT
films						
marking						
high-speed cameras						
optics						
sensitometers						
electronics						
signal generators						
design						
development						
tuning forks						
diodes						
waveforms						